GS2018-8

Tectonic setting of the Gordon gold deposit, Lynn Lake greenstone belt, northwestern Manitoba (parts of NTS 64C16): evidence from lithogeochemistry, Nd isotopes and U-Pb geochronology

by X.M. Yang and C.J.M. Lawley[1]

In Brief:

- Supracrustal rocks in the Farley Lake area formed in an island-arc to back-arc setting with depleted-mantle sourced volcanism
- Tectonic evolution is reflected by granitoid intrusions ranging from arc, I-type; intra-arc, extension-related, A-type; to late adakite-like
- The latter are ca. 1854 Ma and provide important structural-chemical controls for localization of auriferous vein systems

Citation:
Yang, X.M. and Lawley, C.J.M. 2018: Tectonic setting of the Gordon gold deposit, Lynn Lake greenstone belt, northwestern Manitoba (parts of NTS 64C16): evidence from lithogeochemistry, Nd isotopes and U-Pb geochronology; *in* Report of Activities 2018, Manitoba Growth, Enterprise and Trade, Manitoba Geological Survey, p. 89–109.

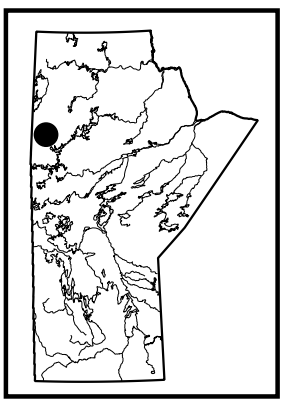

Summary

This report combines new lithogeochemical and Nd isotopic data with previously reported U-Pb zircon geochronological data for supracrustal and intrusive rocks at the Gordon Au deposit in the Farley Lake area, northern part of the Paleoproterozoic Lynn Lake greenstone belt, northwestern Manitoba. Auriferous veins are hosted primarily in unit 4 banded iron formation, which represents part of an interflow sedimentary succession that is coeval with volcanic and volcaniclastic rocks and was intruded by a series of distinct granitoid suites. The volcanic and volcaniclastic rocks (units 1 to 3) share geochemical similarities with modern island-arc volcanic rocks, whereas marine sedimentary rocks intercalated with lesser volcaniclastic rocks (unit 4) were likely deposited in a back-arc setting.

Recent, sensitive high-resolution ion microprobe (SHRIMP) U-Pb zircon ages, together with new lithogeochemical results, establish the following sequence of granitoid magmatism: 1) ca. 1879 Ma, pre–Sickle group, arc, I-type granodiorite-monzogranite (unit 6); 2) ca. 1872 Ma, A-type, alkali-feldspar granite to syenogranite (unit 7) with intra-arc extensional affinity; and 3) ca. 1854 Ma, syn– to post–Sickle group, quartz diorite to monzodiorite (unit 8) formed in a syn- to late-accretionary environment. Quartz diorite samples yielded compositional characteristics that resemble adakites and/or sanukitoids, suggesting derivation from partial melting of previously metasomatized, sub-arc lithospheric mantle. Quartz diorite is coeval with the ca. 1.85 Ga Wathaman-Chipewyan batholith, which marks the terminal, accretionary collision of the Lynn Lake greenstone belt and the Hearne craton to the north. Auriferous veins hosted by pre– to syn–peak metamorphic D_2 faults and related splays, as well as favourable hostrocks (i.e., unit 4 banded iron formation, and units 2 and 3 iron-rich, tholeiitic volcanic and volcaniclastic rocks) that destabilized Au-S complexes within hydrothermal fluids, represent the two dominant ore-system controls.

Adakite-like intermediate intrusions at 1854 Ma significantly predate metamorphic ages and auriferous veins in the Lynn Lake greenstone belt (ca. 1810–1780 Ma). The cospatial relationship between Au deposits and the ca. 1.85 Ga suite, however, suggests that the structural architecture that was later reactivated by auriferous veins was established prior to the continent-continent collision between the composite Hearne and Superior cratons at ca. 1.80 Ga. A similar spatial association between the ca. 1.85 Ga magmatic suite and structures is also documented at the MacLellan Au-Ag deposit (i.e., the 1857 Ma Burge Lake pluton), suggesting that intrusions of this suite may demarcate favourable lithological assemblages and/or structural architecture as main controls for Au deposits.

Introduction

In 2018, the Manitoba Geological Survey (MGS) continued its multiyear bedrock mapping project in the Paleoproterozoic Lynn Lake greenstone belt (LLGB) of northwestern Manitoba (Figure GS2018-8-1). So far, three preliminary maps at 1:20 000 scale have been published by the MGS to cover type areas around the MacLellan Au-Ag, Gordon Au (formerly known as the Farley Lake mine) and Burnt Timber Au mines (Yang and

[1] Natural Resources Canada, Geological Survey of Canada, 601 Booth Street, Ottawa, ON K1A OE8

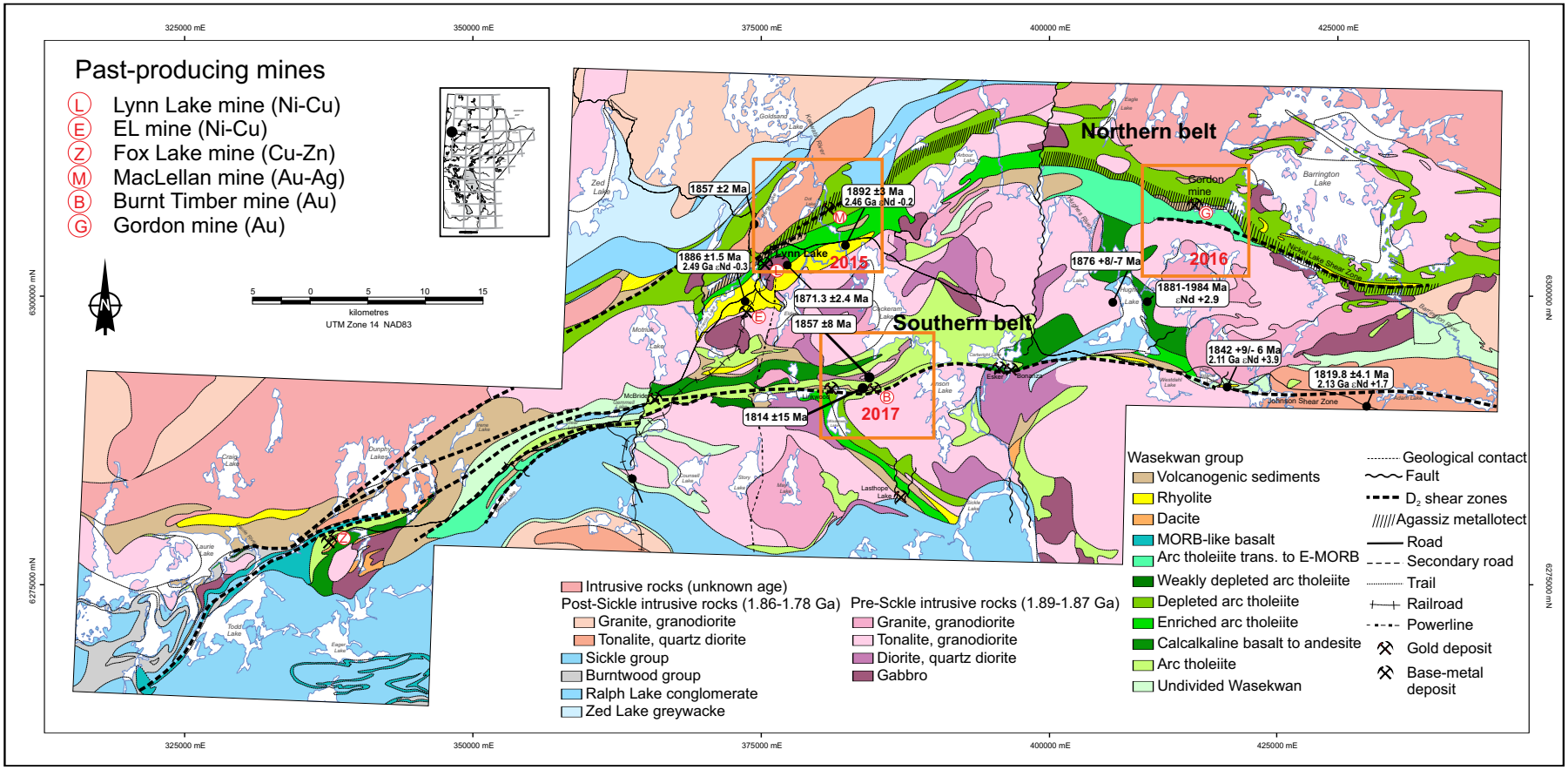

Figure GS2018-8-1: *Regional geology of the Lynn Lake greenstone belt, with U-Pb zircon ages and Nd isotopic compositions (modified and compiled from Gilbert et al., 1980; Manitoba Energy and Mines, 1986; Gilbert, 1993; Zwanzig et al., 1999; Turek et al., 2000; Beaumont-Smith and Böhm, 2002, 2003, 2004; Beaumont-Smith et al., 2006; Beaumont-Smith, unpublished data, 2006; Beaumont-Smith, 2008). Updated, detailed mapping areas at 1:20 000 scale are indicated by the orange boxes, including that surrounding the Gordon Au deposit (labelled 'G'). Abbreviations: MORB, mid-ocean–ridge basalt; E-MORB, enriched MORB; Trans., transitional.*

Beaumont-Smith, 2015, 2016a, 2017). These studies have identified favourable supracrustal rock successions, multiple suites of granitoid intrusions and structural-chemical controls important for localizing Au mineralization. The study of Au mineralization and its relationship with granitoid intrusions, regional metamorphism and structures is ongoing via collaborative research between the MGS and the Geological Survey of Canada (GSC) under Phase 5 of their Targeted Geoscience Initiative program (TGI-5). This report focuses on the timing and composition of magmatic and supracrustal rocks, tectonic implications for magmatism and their genetic relationship to Au mineralization.

This study combines new lithogeochemistry (n = 59 samples) and Nd-isotope (n = 6) datasets with previously published sensitive high-resolution ion microprobe (SHRIMP) U-Pb zircon ages (n = 3; Lawley et al., 2018) for the rock units of the Gordon Au deposit in the Farley Lake area. Together, the data provide geochemical and geochronological constraints to distinguish multiple magmatic suites, unravel the petrogenetic history of supracrustal and intrusive rocks, provide tectonic implications and explore the relationship between magmatism and Au metallogeny.

This report assigns diorite, quartz diorite and minor gabbroic rocks, defined by Yang and Beaumont-Smith (2016a, 2016b) as unit 6b, to a new unit 8 on the basis of SHRIMP U-Pb zircon age data (Lawley et al., 2018), and identifies the presence of arc I-type granitoids; intra-arc, extension-related, A-type granites; and late-orogenic, adakite-like quartz diorites. These intrusive rocks are interpreted to represent diverse tectonic settings, which would provide new insights into the tectonic evolution and Au metallogeny of the Farley Lake area.

General geology

The LLGB (Bateman, 1945) is a major tectonic element of the internal Reindeer zone of the Trans-Hudson orogen (Stauffer, 1984; Lewry and Collerson, 1990), which is the largest Paleoproterozoic orogenic belt of Laurentia (Hoffman, 1988; Corrigan et al., 2007, 2009). The LLGB is bounded to the north by the Southern Indian domain, composed of variably migmatitic metasedimentary rocks, various granitoids and minor metavolcanic rocks (Kremer et al., 2009). Synorogenic basins, including the Kisseynew metasedimentary domain, represent the southern limit of the LLGB (Gilbert et al., 1980; Fedikow and Gale, 1982; Syme, 1985; Zwanzig et al., 1999; Beaumont-Smith and Böhm, 2004; Zwanzig and Bailes, 2010). Paleoproterozoic greenstone belts with ages and lithological assemblages similar to the LLGB occur to the east (Rusty Lake belt), to the west (La Ronge belt) and to the far south (Flin Flon belt; e.g., Ansdell et al., 1999; Park et al., 2002; Ansdell, 2005; Corrigan et al., 2007, 2009; Glendenning et al., 2015; Hastie et al., 2018).

The LLGB consists of two east-trending, steeply dipping belts that contain various supracrustal rocks, known locally as the Wasekwan group (Bateman, 1945; Gilbert et al., 1980), along with younger molasse-type sedimentary rocks that constitute the Sickle group (Figure GS2018-8-1; Norman, 1933). The southern and northern belts are separated by granitoid plutons of the 1.89–1.87 Ga Pool Lake intrusive suite (Figure GS2018-8-1; Gilbert et al., 1980; Baldwin et al., 1987). In the central and southern parts of the LLGB, the Sickle group overlies the Wasekwan group and felsic–mafic plutonic rocks of the Pool Lake intrusive suite along an angular unconformity. The Sickle group correlates well with the 1850–1840 Ma MacLennan group in the La Ronge greenstone belt in Saskatchewan in terms of composition, stratigraphic position and contact relationships (Ansdell et al., 1999; Ansdell, 2005). Cutting the entire LLGB are the much younger Mackenzie dikes (ca. 1267 Ma; Baragar et al., 1996), as indicated by regional aeromagnetic data, that appear to truncate volcanic and plutonic rocks folded during peak metamorphism at 1.81–1.80 Ga.

Significant differences in the geology and geochemistry of the northern and southern belts in the LLGB may reflect regional differences in tectonic settings that are obscured by structural transposition and imbrication during multiple stages of deformation (Gilbert et al., 1980; Syme, 1985; Zwanzig et al., 1999). This complexity leads to the suggestion that the term 'Wasekwan group' should be abandoned because it contains disparate volcanic assemblages that were later structurally juxtaposed during the evolution of the LLGB (Zwanzig et al., 1999), and thus may represent a tectonic collage similar to that described in the Flin Flon greenstone belt (e.g., Stern et al., 1995). However, this report retains the term 'Wasekwan group' to maintain consistency with previous LLGB-related literature.

The Farley Lake area, including the Gordon Au deposit, is situated in the northern belt of the LLGB (Figure GS2018-8-1) and consists mostly of Wasekwan group supracrustal rocks intruded by plutons of the Pool Lake intrusive suite and late intrusive suite (Gilbert et al., 1980; Yang and Beaumont-Smith, 2016a, 2016b; Figure GS2018-8-2). Following the convention of previous workers (e.g., Milligan, 1960; Beaumont-Smith and Böhm, 2004), the intrusions cutting the Wasekwan group (i.e., the Pool Lake intrusive suite of Gilbert et al., 1980) and

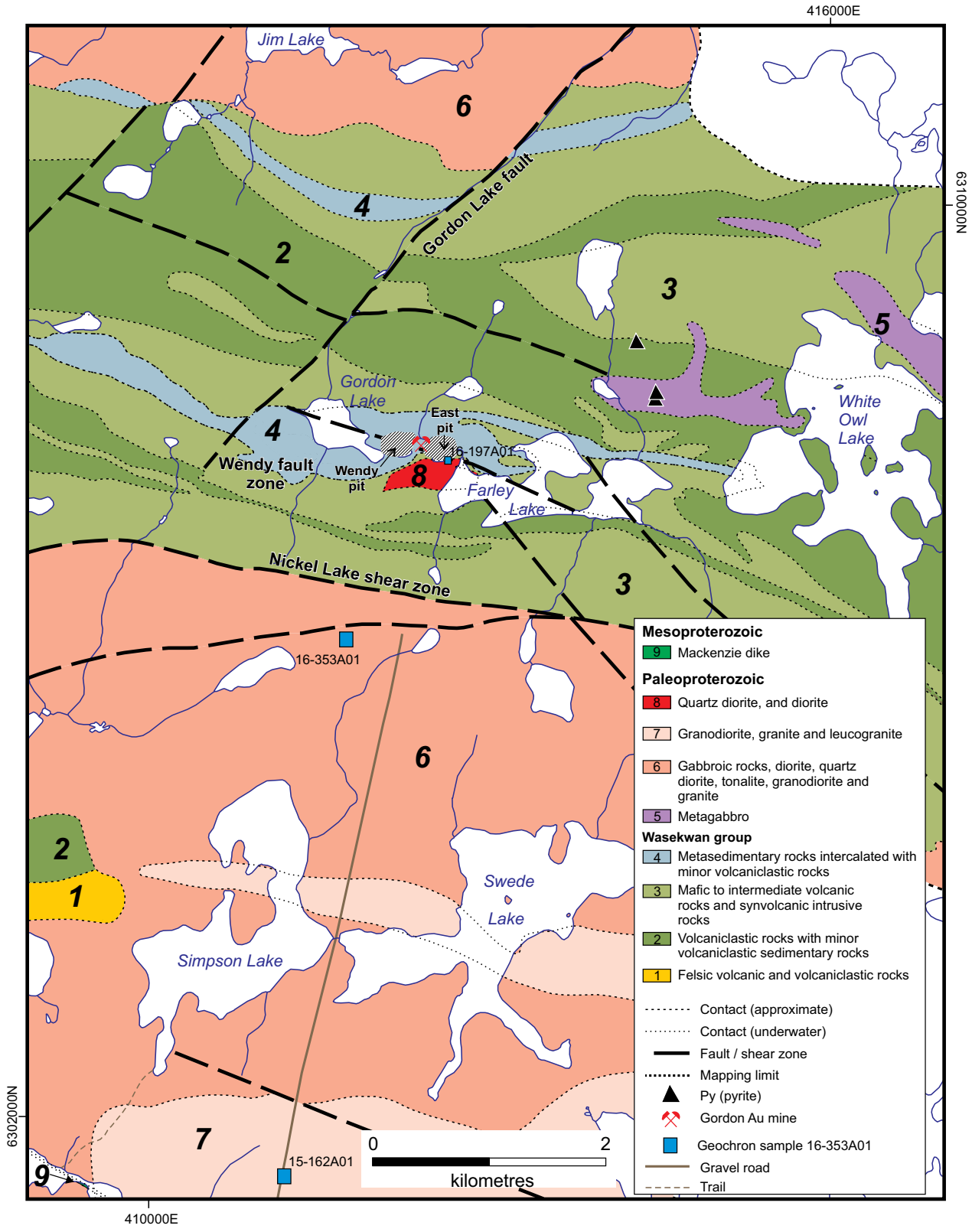

***Figure GS2018-8-2**: Simplified geology of the Farley Lake area, Lynn Lake greenstone belt, northwestern Manitoba (modified from Yang and Beaumont-Smith, 2016a, b). Note: prefix '111' of geochronology sample number is omitted to fit the available space.*

those cutting the Sickle group are called, respectively, the pre-Sickle and post-Sickle suites. Both igneous suites are cut by a late intrusive suite (Yang and Beaumont-Smith, 2015, 2016a, b, 2017) that has an uncertain relationship to the youngest Paleoproterozoic magmatic phase of small pegmatitic and tonalitic intrusions at 1.8–1.78 Ga. A diabase dike interpreted as part of the Mackenzie swarm (ca. 1267 Ma; Baragar et al., 1996) cuts across the southwest corner of the Farley Lake area, as indicated by regional aeromagnetic data. This Mackenzie dike is not further discussed in this report because it is Mesoproterozoic in age and not related to Au metallogeny in the LLGB.

Bedrock mapping in the Farley Lake area in 2016 defined eight map units, including 17 subunits (see Yang and Beaumont-Smith, 2016a, b). Recent SHRIMP U-Pb zircon age data (Lawley et al., 2018) and data presented in this study (see below) suggest that the unit 6b (diorite, quartz diorite and minor gabbroic rocks) defined and described by Yang and Beaumont-Smith (2016a, b) should be changed to a new map unit 8 (Table GS2018-8-1; Figure GS2018-8-2).

It is noted that the supracrustal rocks in the Farley Lake map area, similar to others in the LLGB, were metamorphosed to greenschist to amphibolite facies (Gilbert et al., 1980; Beaumont-Smith and Böhm, 2004; Yang and Beaumont-Smith, 2015, 2016a, 2017); however, for brevity, the prefix 'meta' is omitted in this report. In the following section, the geochemical characteristics of major rock types from different map units are described to determine their magmatic affinities.

Lithogeochemistry

This report compiles geochemical data on 59 whole-rock samples from the Farley Lake area, including 46 samples from this study [note: analyses were carried out using the 4Litho package at Activation Laboratories Ltd. in Ancaster, Ontario; detailed analytical procedures and methods were described in Anderson (2013)], seven from Zwanzig et al. (1999), five from D. Peck (unpublished data, 1999) and one from Beaumont-Smith (2008). Based on the sample locations and/or lithologies, these samples are attributed to the map units defined by Yang and Beaumont-Smith (2016a, b). The major geochemical characteristics are summarized and discussed below for supracrustal (units 1 to 4) and intrusive rocks (units 5 to 8), respectively. Detailed rock descriptions of the different units can be found in Yang and Beaumont-Smith (2016a).

Supracrustal rocks (units 1 to 4)

Classification

Based on the total alkalis versus silica diagram (TAS; Le Bas et al., 1986), seven samples collected from unit 1 felsic to intermediate volcanic and volcaniclastic rocks (Table GS2018-8-1) plot within the fields of andesite, dacite and rhyolite (Figure GS2018-8-3a). Nine samples taken from unit 2 volcaniclastic rocks largely fall into the fields of basalt and basaltic andesite. Nineteen samples from unit 3 mafic to intermediate volcanic rocks plot in the basalt, basaltic andesite and andesite fields. These volcanic and volcaniclastic rocks are dominantly subalkaline (Figure GS2018-8-3a), consistent with the commonly seen volcanic-arc array comprising basalt, andesite and dacite to rhyolite (BADR; Yang and Beaumont-Smith, 2015, 2016a). Based on the calculation of the Rittmann Serial Index σ (= $[Na_2O+K_2O]^2/[SiO_2–43]$, values in wt.%; see Rittmann, 1973), these subalkaline rocks have σ values ranging from 0.39 to 3.06, which can further subdivide them into calcic (tholeiitic) to calcalkaline series (see Yang, 2007), consistent with the studies of Syme (1985) and Zwanzig et al. (1999).

As a comparison, six samples taken from unit 4 sedimentary rocks are also plotted on the TAS diagram (Figure GS2018-8-3a), with two argillite samples (unit 4a) falling into the fields of basaltic andesite and dacite, and four banded iron formation (BIF; unit 4b) samples characterized by very low alkalis (Na_2O+K_2O <0.45 wt.%) and a large range in silica content.

The use of high-field-strength element (HFSE) ratios, such as Zr/TiO_2 and Nb/Y, to classify volcanic and volcaniclastic rocks from units 1 to 3 (Figure GS2018-8-3b) yielded a result similar to the TAS diagram. The HFSEs are commonly considered immobile during hydrothermal alteration and metamorphism up to upper amphibolite facies (Syme, 1985; Rollinson, 1993; Pearce, 1996; Glendenning et al., 2015), thus potentially reflecting the primary compositional characteristics of the supracrustal rocks. All samples have low Nb/Y ratios (<0.7), typical of subalkaline rocks, and low to moderate Zr/TiO_2 ratios, consistent with predominantly mafic to intermediate bulk compositions (Figure GS2018-8-3b; Pearce, 1996).

Rare-earth element patterns

Chondrite-normalized rare-earth element (REE) patterns of units 1 to 4 supracrustal rocks are presented in Figure GS2018-8-4. Unit 1 andesitic to rhyolitic samples display slight light-REE (LREE) enrichment patterns, which are subdivided into felsic and intermediate volcanic rocks, respectively. The former have higher REE

Table GS2018-8-1: Lithostratigraphic units of the Farley Lake area, Lynn Lake greenstone belt, northwestern Manitoba (modified from Yang and Beaumont-Smith, 2016a, b).

Unit	Rock type	Affiliation
9	Diabase of Mackenzie dike (ca. 1267 Ma[1])	Mackenzie dike
	Intrusive contact	
8	Diorite, quartz diorite (1854.4 ±2.4 Ma[2]) and minor gabbroic rocks	Post-Sickle intrusive suite
	Intrusive contact	
7	Granodiorite, granite and leucogranite	Pre-Sickle intrusive suite
7a	Granite and leucogranite (1872.6 ±2.5 Ma[2])	
7b	Granodiorite	
6	Gabbroic rocks, diorite, quartz diorite, tonalite, granodiorite and granite (1879.4 ±4.3 Ma[2]), and associated pegmatic and aplitic dikes	
6a	Tonalite, granodiorite and granite, and associated pegmatic and aplitic dikes	
5	Gabbro and minor diorite	
	Intrusive contact	
4	Sedimentary rocks intercalated with minor volcaniclastic rocks	Wasekwan group
4a	Argillite, metasiltstone and metagreywacke	
4b	Banded iron formation	
4c	Volcaniclastic mudstone, volcaniclastic siltstone and volcaniclastic sandstone	
	Structural contact	
3	Mafic to intermediate volcanic rocks and synvolcanic intrusive rocks	
3a	Diabase and leucogabbroic dikes	
3b	Porphyritic basaltic andesite	
3c	Plagioclase-phyric basalt and aphyric basalt	
3d	Mafic autobreccia	
	Structural contact	
2	Volcaniclastic rocks with minor volcaniclastic sedimentary rocks	
2a	Felsic lapilli tuff and tuff	
2b	Intermediate lapillistone, lapilli tuff and tuff	
2c	Mafic lapillistone, mafic lapilli tuff, tuff and minor mafic mudstone	
2d	Mafic tuff breccia and breccia	
	Structural contact	
1	Felsic volcanic and volcaniclastic rocks: rhyolite, dacite and felsic to intermediate volcaniclastic rocks	
1a	Rhyolite, and dacite (1884 to 1881 Ma[3])	
1b	Felsic to intermediate volcaniclastic rocks	
	Basement?	

[1] Baragar et al. (1996)
[2] Lawley et al. (2018) - summarized in this study
[3] Beaumont-Smith (unpublished data, 2006)

abundance with notable negative Eu anomalies, whereas the latter have lower REE concentrations with a slightly positive Eu anomaly (Figure GS2018-8-4a). Unit 2 basaltic to andesitic volcaniclastic rocks are similarly subdivided into basaltic and andesitic volcaniclastic rocks, respectively. The basaltic group exhibits a flat REE pattern, low REE contents and slightly positive Eu anomalies. The andesitic group, in comparison, has slightly enriched REE patterns, higher REE abundances and no or slightly negative Eu anomalies (Figure GS2018-8-4b).

Unit 3 basalt to andesite samples display varied REE patterns: mafic samples have flat REE profiles with notable positive Eu anomalies, whereas intermediate samples are variably LREE enriched with flat to slightly negative Eu anomalies (Figure GS2018-8-4c). Rare-earth element patterns for unit 3 samples are typical of basaltic to andesitic

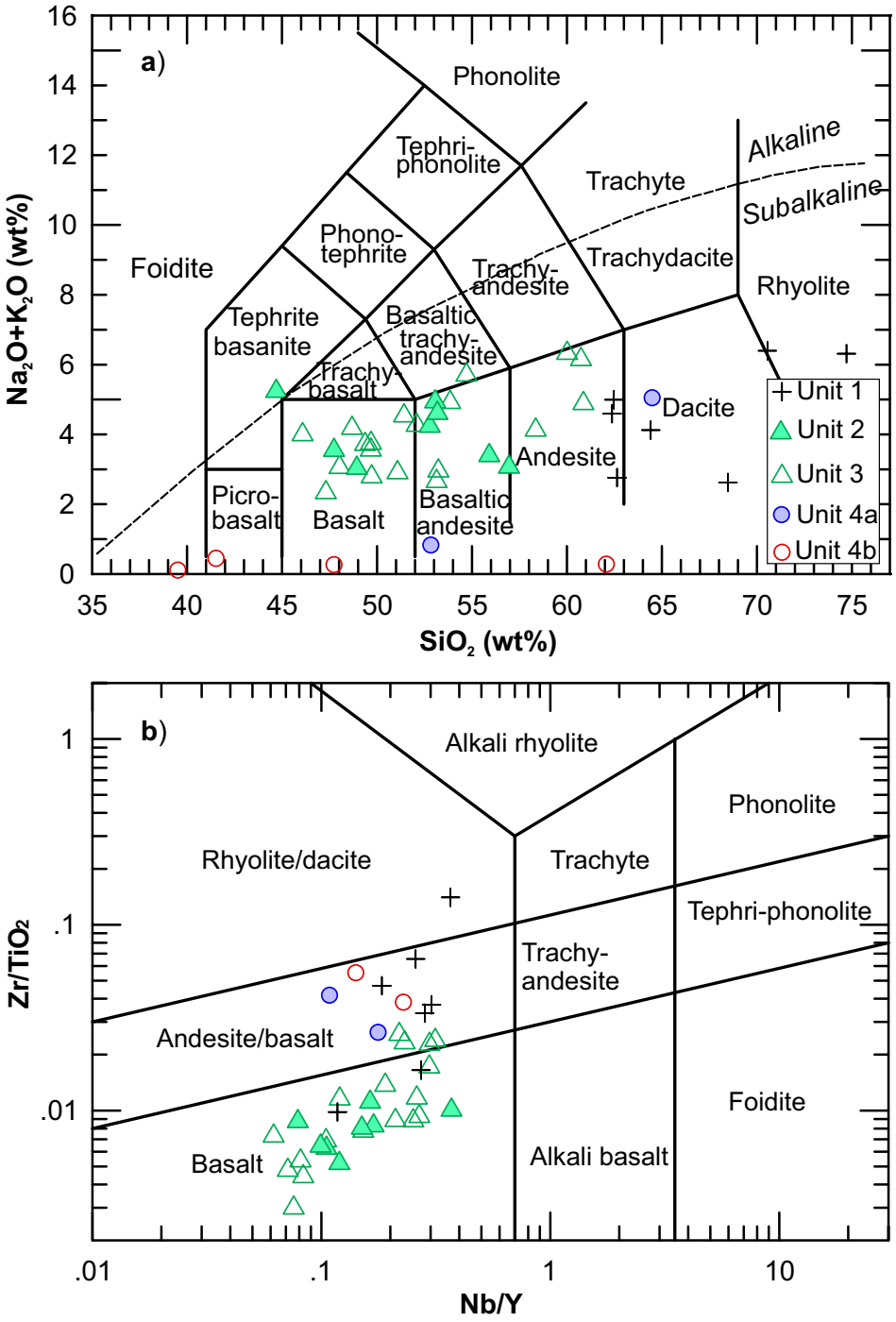

Figure GS2018-8-3: *Geochemical classification of supracrustal rocks from the Farley Lake area:* ***a)*** *total alkalis (Na_2O+K_2O; wt.%) versus SiO_2 (wt.%) diagram (TAS; after Le Bas et al., 1986); dashed line is the boundary between the subalkaline and alkaline series (after Irvine and Baragar, 1971);* ***b)*** *Zr/TiO_2 versus Nb/Y (after Pearce, 1996).*

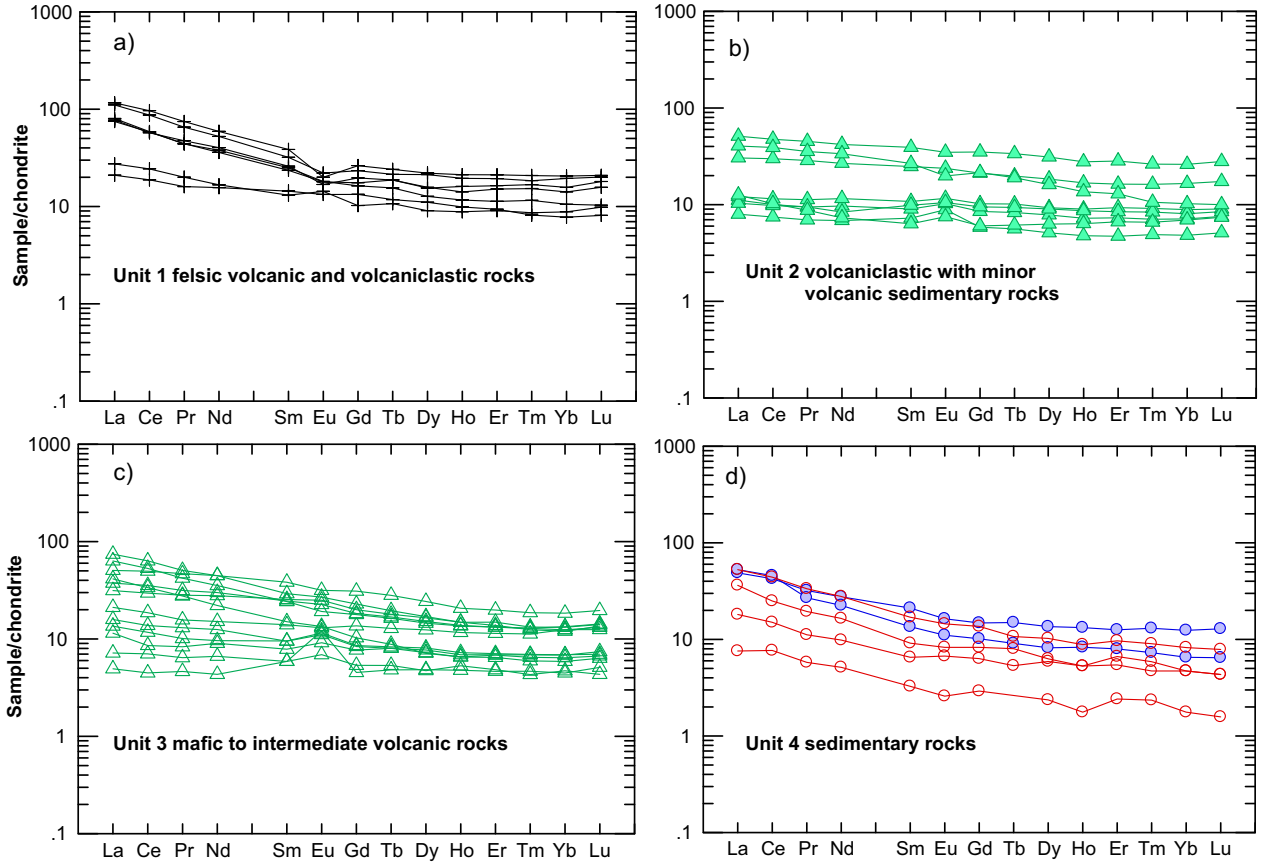

Figure GS2018-8-4: *Chondrite-normalized rare-earth element (REE) patterns of units 1 to 4 supracrustal rocks from the Farley Lake area. Normalizing values from Sun and McDonough (1989). Symbols as in Figure GS2018-8-3. Argillite samples in blue.*

volcanic rocks formed in volcanic-arc settings, consistent with the results of tectonic discrimination diagrams using HFSE systematics (e.g., Zr-Th-Nb [Wood, 1980] and Nb-Zr-Y [Meschede, 1986] ternary plots, not shown).

Unit 4 sedimentary samples display LREE-enriched distribution patterns with no or very subtle Eu anomalies, similar to units 2 and 3 volcanic and volcaniclastic samples. Argillite samples (in blue) have slightly higher REE abundances than the BIF samples (Figure GS2018-8-4d). Interestingly, unit 4 sedimentary samples have a volcanic-arc signature using the Zr-Th-Nb-Y systematics (Wood, 1980; Meschede, 1986). This suggests that unit 4 sedimentary rocks may have been derived, at least in part, from volcanic-arc or island-arc rocks (e.g., Frisch et al., 2011).

Extended trace-element patterns

On primitive-mantle–normalized, extended trace-element plots, unit 1 andesitic to rhyolitic samples can be subdivided into two groups, both of which display pronounced negative Nb, Ta and Ti anomalies (Figure GS2018-8-5a). Andesitic samples have lower trace-element concentrations (i.e., <10 times normalizing values) compared to the dacite to rhyolite samples. The negative Nb anomalies exhibited by unit 1 volcanic rocks are typical of volcanic-arc environments that sequester some HFSE within high-pressure rutile during subduction (cf. Pearce and Peate, 1995; Pearce, 2008).

Unit 2 basaltic to andesitic volcaniclastic rocks exhibit fairly flat extended trace-element profiles (Figure GS2018-8-5b), with subtle negative Nb, Ta and Ti anomalies relative to unit 1. A few samples lack such anomalies, which may be due to the presence of magnetite porphyroblasts (Yang and Beaumont-Smith, 2016a) that are commonly enriched in Nb, Ta, and Ti (cf. Rollinson, 1993) and/or, in the case of volcaniclastic rocks, less contamination from felsic detritus.

Unit 3 basalt and basaltic andesite to andesite samples have varied trace-element abundances, ranging from <1 to ~20 times normalizing values (Figure GS2018-8-5c). These volcanic rocks show a typical arc-like signature, manifested by the presence of negative Nb, Ta, and Ti anomalies, although a few magnetite-bearing samples do not have such pronounced anomalies. It was noticed that Ta contents in seven samples from Zwanzig et al.

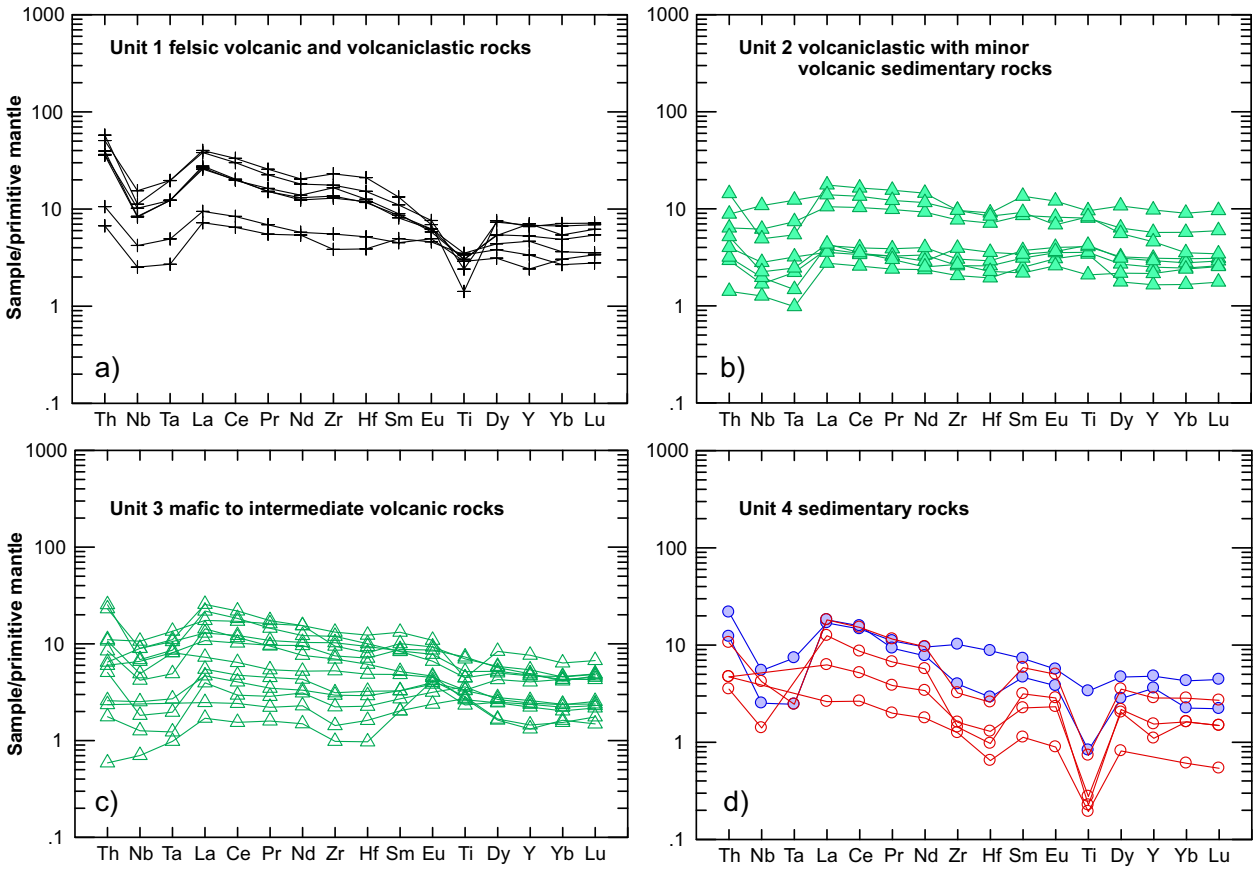

Figure GS2018-8-5: *Primitive-mantle–normalized spider diagram for units 1 to 4 supracrustal rocks. Normalizing values from Sun and McDonough (1989). Symbols as in Figure GS2018-8-3.*

(1999) are anomalously high; these samples were prepared using a tungsten carbide mill, leading to artificially elevated Ta and W contents, whereas other elements were not affected (S. Gagné, pers. comm., 2018). Thus, these seven samples were not plotted in Figure GS2018-8-5c.

Unit 4 sedimentary rocks show a very strong arc signature with pronounced negative Nb, Ta and Ti anomalies (Figure GS2018-8-5d), suggesting that they may have been sourced from arc rocks. Also, most of the sedimentary samples display negative Zr and Hf anomalies (Figure GS2018-8-5d), likely reflecting a provenance lacking in zircon.

Intrusive rocks (units 5 to 8)

Classification

Four samples of unit 5 medium-grained gabbro plot in the quartz gabbro and diorite fields of the CIPW normative Q' versus ANOR classification by Streckeisen and Le Maitre (1979) in Figure GS2018-8-6.

Geochemically, unit 5 gabbroic rocks evolved from magnesian to ferroan affinity, and belong to the calcic to calc-alkali series (Figure GS2018-8-7a, b). The Fe-rich affinity of unit 5 samples is consistent with their σ values ranging from 1.25 to 2.42, which is typical of calcalkaline volcanic-arc rocks (Yang, 2007). Unit 5 samples have aluminum saturation index (ACNK = molar ratio Al/(Ca+Na+K); see Maniar and Piccoli, 1989) values of 0.67 to 0.84, indicating that they are metaluminous.

Unit 6 granitoids occur widely in the Farley Lake area (Figure GS2018-8-2), with a large range of lithologies (Table GS2018-8-1; see Yang and Beaumont-Smith, 2016a for detailed descriptions). Seven whole-rock samples collected from unit 6 vary from quartz diorite, tonalite and granodiorite to monzogranite (Figure GS2018-8-6). The Unit 6 samples are magnesian to ferroan, calcic to calcalkaline and predominantly peraluminous (Figure GS2018-8-7a–c). These granitoid rocks display σ values of 0.99 to 1.32, evolving along the trend of calcic to calcalkalic (Figure GS2018-8-6) that is typical of volcanic-arc–like, calcalkaline granitoid rocks (Yang, 2007; Whalen and Frost, 2013).

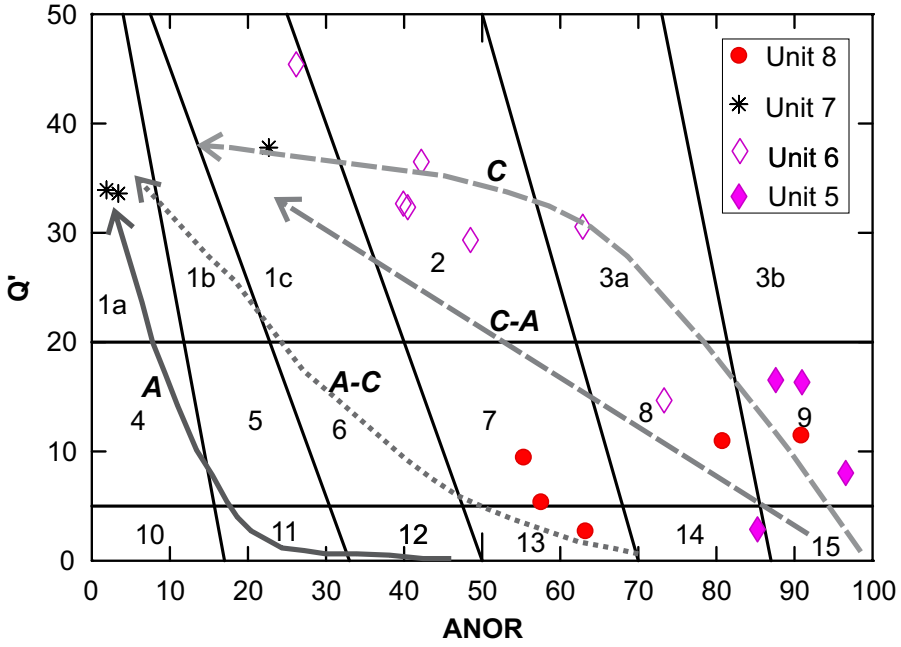

Figure GS2018-8-6: *Classification of units 5 to 8 intrusive rocks from the Farley Lake area, based on the CIPW normative Q' vs. ANOR diagram of Streckeisen and Le Maitre (1979). Q' = CIPW normative 100*qz/(qz+or+ab+an); ANOR = CIPW normative 100*an/(an+or). Rock units: 1a, alkali-feldspar granite; 1b, syenogranite; 1c, monzogranite; 2, granodiorite; 3a, tonalite; 3b, calc tonalite; 4, alkali-feldspar quartz syenite; 5, quartz syenite; 6, quartz monzonite; 7, quartz monzodiorite; 8, quartz diorite; 9, quartz gabbro; 10, alkali-feldspar syenite; 11, syenite; 12, monzonite; 13, monzogabbro; 14, diorite; 15, gabbro. Coarse dashed and solid lines with arrows indicate interpreted differentiation trends of different magmatic suites (after Whalen and Frost, 2013): C, calcic; C-A, calcalkali; A-C, alkali-calcic; A, alkali. Abbreviations: ab, albite; an, anorthite; or, orthoclase; qz, quartz.*

Voluminous bodies of unit 6 granitoids are I-type, based on their mineral assemblage (amphibole, biotite, magnetite), and were likely emplaced in a juvenile to mature island-arc setting (e.g., Rudnick and Gao, 2003; Arndt, 2013).

Unit 7 granite samples are highly evolved in chemical composition, with silica contents of 75.33 to 77.86 wt.% and Mg# [molar 100×MgO/(MgO+FeO^{tot})] of 2 to 37. Three unit 7 granite samples plot in the fields of alkali-feldspar granite and monzogranite (Figure GS2018-8-6) but are compositionally diverse (Figure GS2018-8-7a–c). The chemical variability of unit 7 may reflect grouping of at least two disparate rock types and/or magmatic differentiation of A-type granites (e.g., Eby, 1990) emplaced in an intra-arc extensional setting (see below).

Unit 8 granitoid samples, as defined in this study by SHRIMP U-Pb zircon age determination, occur as a small stock at the south edge of the Gordon Au deposit (Figure GS2018-8-2) that was previously mapped as part of unit 6b in Yang and Beaumont-Smith (2016a, b). Five unit 8 granitoid samples display a compositional range from quartz monzodiorite and quartz diorite to quartz gabbro and monzogabbro in the CIPW normative Q' versus ANOR classification diagram (Figure GS2018-8-6). These rocks have a relatively narrow range and moderate silica contents of 51.46 to 58.62 wt.%, high Al_2O_3 of 15.37 to 16.99 wt.% and moderate to high Mg# of 52 to 60. The mafic to intermediate rocks included within unit 8 are exclusively magnesian, alkali-calcic (except for one calcic sample) and metaluminous. They have σ values ranging from 2.44 to 3.58, attributed mostly to the calcalkaline to alkaline series, albeit one sample (σ = 0.95) is calcic (tholeiitic).

REE patterns

Chondrite-normalized REE patterns of units 5 to 8 intrusive rocks are presented in Figure GS2018-8-8. Unit 5 gabbros have relatively low REE concentrations, approximately 3 to 10.5 times chondrite values. They show flat, undifferentiated REE patterns (low La/Yb ratios of 1.9 to 2.7) with small positive Eu anomalies (Eu*/Eu values of 1.15 to 1.23; Figures GS2018-8-7d and 8a) that may suggest the presence of cumulus plagioclase grains (cf. Rollinson, 1993).

Unit 6 granitoids exhibit enriched REE patterns (La/Yb ratios are 7.3 to 19.9) with marked negative Eu anomalies (Eu*/Eu values of 0.61 to 0.88), except for one sample with a steeply dipping REE profile (La/Yb ratio of 25.1) and a positive Eu anomaly (Eu*/Eu value of 2.16; Figures GS2018-8-7d and -8b), suggesting that plagioclase fractionation prior to emplacement may be a petrogenetic

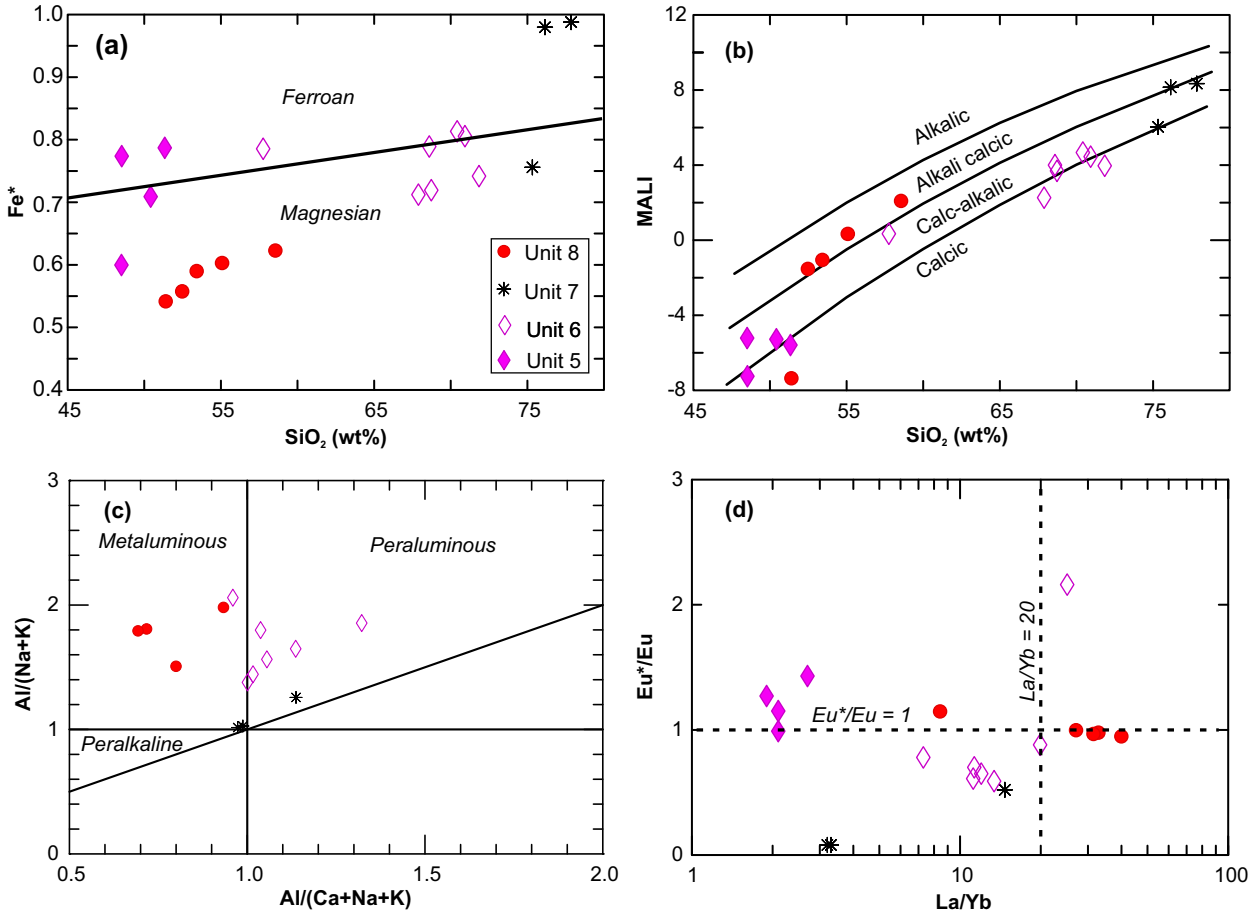

Figure GS2018-8-7: *Geochemical discrimination diagrams for units 5 to 8 intrusive rocks from the Farley Lake area:* ***a)*** *classification of ferroan vs. magnesian granitoids (with fields from Frost et al., 2001); Fe* = $FeO^{tot}/(FeO^{tot}+MgO)$;* ***b)*** *MALI vs. SiO_2 (wt.%); MALI = $Na_2O+K_2O–CaO$ in wt.% (after Frost et al., 2001);* ***c)*** *Shand index (fields from Maniar and Piccoli, 1989); ACNK = $Al_2O_3/(CaO+Na_2O+K_2O)$, A/NK = $Al_2O_3/(Na_2O+K_2O)$, in moles;* ***d)*** *Eu*/Eu vs. La/Yb.*

feature of some unit 6 granitoid plutons (cf. Rollinson, 1993).

Two unit 7 granite samples display flat to slightly enriched REE patterns with pronounced negative Eu anomalies (Figure GS2018-8-8c). These highly evolved granites have La/Yb ratios of 3.2 to 14.7 and Eu*/Eu values of 0.08 to 0.52 (Figure GS2018-8-7d), suggesting that plagioclase may have been involved, either as an early fractionating phase and/or as a residue of its source rocks (e.g., Rollinson, 1993). The third unit 7 sample yielded an REE profile and peraluminous affinity more similar to unit 6 granitoids.

Most quartz diorite and quartz monzodiorite to quartz gabbro samples from unit 8 display strongly LREE-enriched and HREE-depleted patterns without notable Eu anomalies, although one sample yielded relatively lower REE concentrations with a slightly positive Eu anomaly (Figure GS2018-8-8d). These dioritic rocks have high La/Yb ratios of 27.3 to 40.30, and Sr/Y ratios of 45.9 to 55.1, similar to those of adakites or sanukitoids (e.g., Shirey and Hanson, 1984; Stern et al., 1989; Martin et al., 2005; Richards and Kerrich, 2007). One diorite sample (111-16-291A01; see Figure GS2018-8-8d), however, has a La/Yb ratio of 8.5 and Sr/Y ratio of 36.3, atypical of adakites (Richards and Kerrich, 2007).

Extended trace-element patterns

Figure GS2018-8-9 shows primitive-mantle–normalized, extended trace-element profiles for units 5 to 8 intrusive rocks. Unit 5 gabbroic rocks have low HFSE contents, ranging from <1 to 10 times primitive-mantle–normalized values. They display flat trace-element profiles with negative Nb, Ta, Zr and Hf anomalies and slightly positive Ti anomalies (Figure GS2018-8-9a). These HFSE systematics represent a typical arc signature with cumulative phases (e.g., Ti-bearing magnetite), indicative of relatively oxidized magmas. The REE patterns also indicate

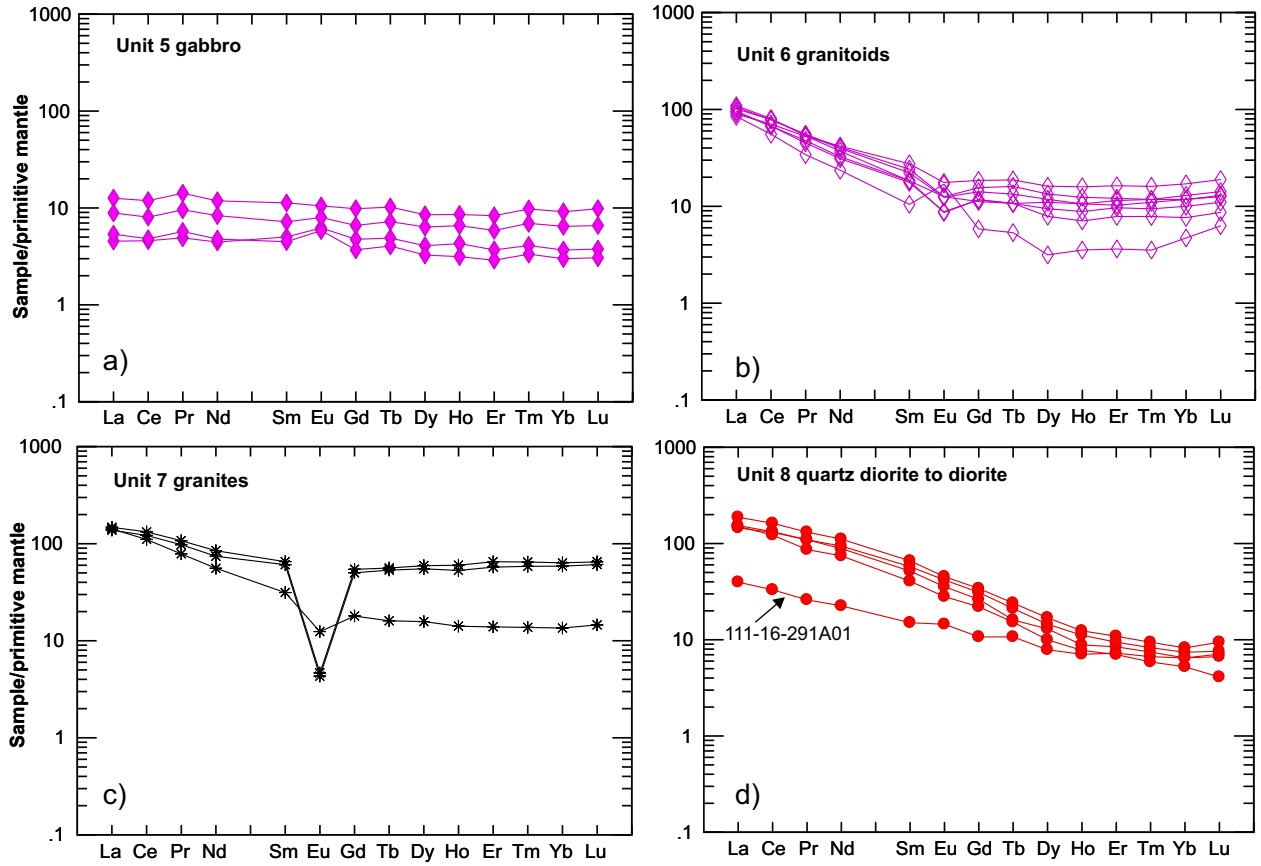

Figure GS2018-8-8: *Chondrite-normalized rare-earth element (REE) patterns of units 5 to 8 intrusive rocks. Normalizing values from Sun and McDonough (1989). Symbols as in Figure GS2018-8-6.*

the presence of cumulate plagioclase in some of the gabbroic rocks of unit 5 (Figure GS2018-8-8c).

Unit 6 granitoid samples display enriched trace-element patterns with negative slopes and pronounced negative Nb, Ta, and Ti anomalies (Figure GS2018-8-9b), suggesting that they may have been emplaced in a magmatic-arc setting. One quartz diorite sample (111-16-292A01) is characterized by positive Ti, Zr, Hf and Eu anomalies suggestive of cumulative phases such as Ti-bearing magnetite, zircon and plagioclase.

Unit 7 granite samples are Th-rich relative to other HFSEs, with pronounced negative Nb and Ti anomalies (Figure GS2018-8-9c). Two alkali-feldspar granite samples are relatively Ta rich, distinct from continental-arc magmatism, and yielded positive Hf anomalies, more typical of an intra-arc extensional environment.

Quartz diorite to quartz monzogabbroic rocks of unit 8 are relatively Th rich and yielded pronounced negative Nb, Ta, Zr, Hf, and Ti anomalies (Figure GS2018-8-9d). The major (MgO rich, moderate SiO_2, Al_2O_3 rich) and trace-element (Y and HREE poor; Sr rich) characteristics of unit 8 samples are similar to those of adakite-sanukitoid rocks, which are interpreted to have been derived from prior metasomatized lithospheric mantle beneath a magmatic arc and/or direct melting of a subducting slab (e.g., Shirey and Hanson, 1984; Stern et al., 1989; Martin et al., 2005).

Tectonic settings

Geochemical characteristics of the supracrustal rocks (units 1 to 4) and intrusive rocks (units 5 to 8) described above document a heterogeneous suite of calcalkaline to tholeiitic, magnesian to ferroan, and metaluminous to moderately peraluminous rocks based on their variable trace-element profiles (Figures GS2018-8-4 to -9). Most of these rocks yielded pronounced negative Nb, Ta and Ti anomalies typical of rocks that formed in an arc-like setting, as was suggested elsewhere in the LLGB (Syme, 1985; Zwanzig et al., 1999). Analyzed rocks from the Farley Lake area, however, are dissimilar to some of the relatively Th-poor and Nb-rich mafic volcanic rocks hosting the MacLellan deposit (Glendenning et al., 2015), except for unit 8 intrusive rocks that yielded a distinct trace-element signature.

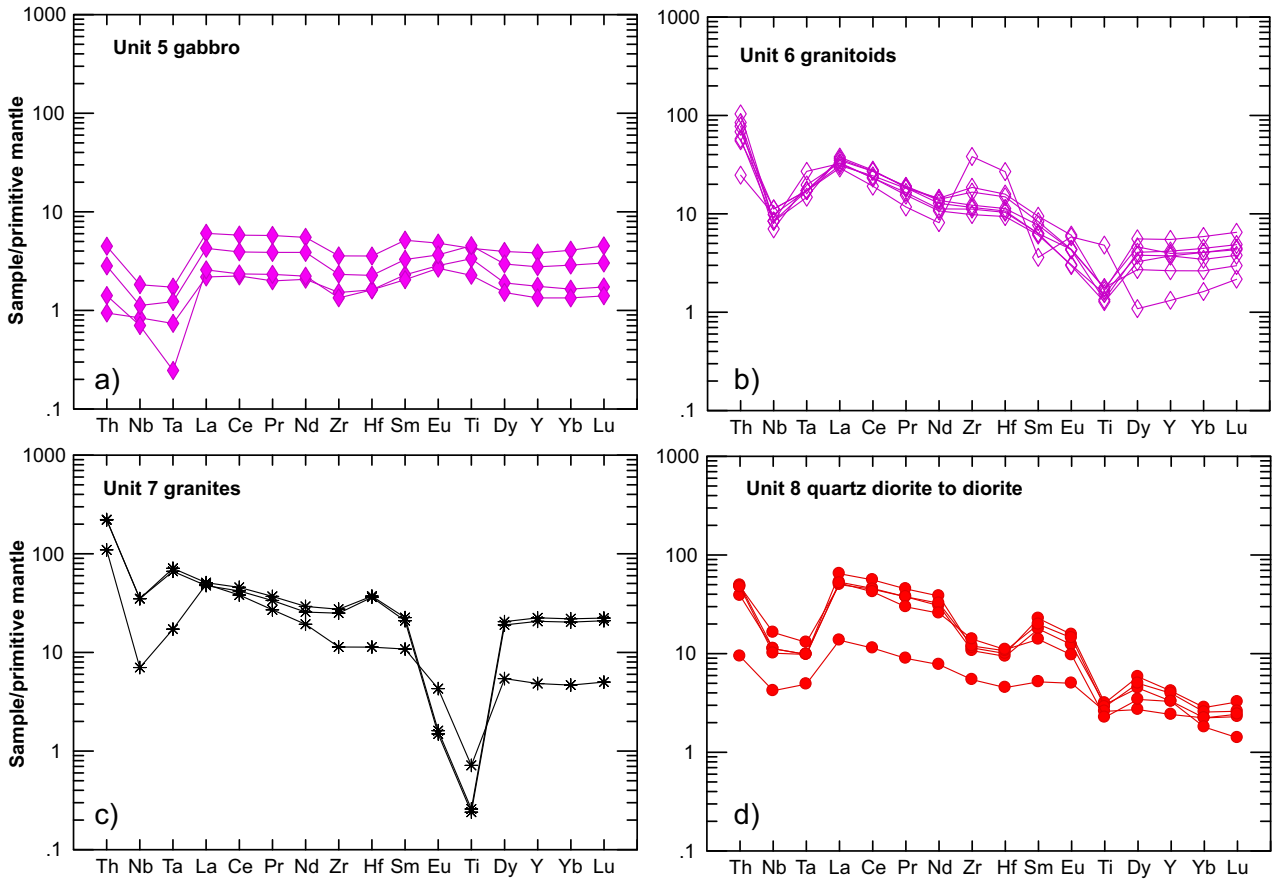

Figure GS2018-8-9: *Primitive-mantle–normalized, extended trace-element patterns of units 5 to 8 intrusive rocks. Normalizing values from Sun and McDonough (1989). Symbols as in Figure GS2018-8-6.*

As a comparison, unit 5 gabbroic rocks are plotted together with units 6 to 8 granitoid rocks in tectonomagmatic discrimination diagrams (Figure GS2018-8-10a, b) to further characterize their tectonic affinity. Samples from units 5, 6 and 8 plot exclusively in the volcanic-arc granitoid field defined by Pearce et al. (1984). Units 5, 6 and 8 rocks are also comparable to arc I-type granitoids, following the approach of Christiansen and Keith (1996). Two unit 7 granite samples, however, fall into the field of within-plate or A-type granites (Figure GS2018-8-10a). Similar results are obtained by using the Zr (ppm) versus 10^4Ga/Al discrimination diagram (not shown) of Whalen et al. (1987). On the Hf–Rb/30–Ta*3 ternary discrimination diagram (Figure GS2018-8-10b; Harris et al., 1986), unit 7 granites are located in the field of within-plate granites, whereas units 5, 6 and 8 samples plot mostly in the volcanic-arc and within-plate granite fields. Magmatic suites, therefore, seem to represent a complex assemblage of granitoid rock types, with each geochemical composition reflecting the complex interplay between magmatic processes, source compositions and tectonic settings.

Sm-Nd geochemical and isotopic systematics

In order to obtain isotope geochemical information on the nature and evolution of volcanic rocks in the Farley Lake area, six volcanic samples from map units 1a, 3b, and 3c (Table GS2018-8-1) were selected for Sm-Nd isotopic analysis at the University of Alberta. Detailed analytical procedures followed the approach described in Böhm et al. (2007) and Anderson (2013). The analytical results are listed in Table GS2018-8-2.

The Sm/Nd ratios range from 0.21 to 0.29 (average 0.26) and tend to decrease with increasing silica content (i.e., 0.28 to 0.29 in unit 3c basalt, 0.22 to 0.29 in unit 3b andesite and 0.21 in unit 1a rhyolite; Table GS2018-8-2). The systematic variation of Sm/Nd ratios with rock type is consistent with magmatic differentiation. We note that the Sm/Nd ratios of the Farley Lake volcanic samples are higher than the upper continental crust (0.19; see Goldstein et al., 1984) and average continental crust (0.195; Rudnick and Gao, 2003) but lower than the primitive mantle (0.33) and N-type MORB (0.36; Sun and McDonough, 1989). Basaltic Sm/Nd ratios from unit 3c

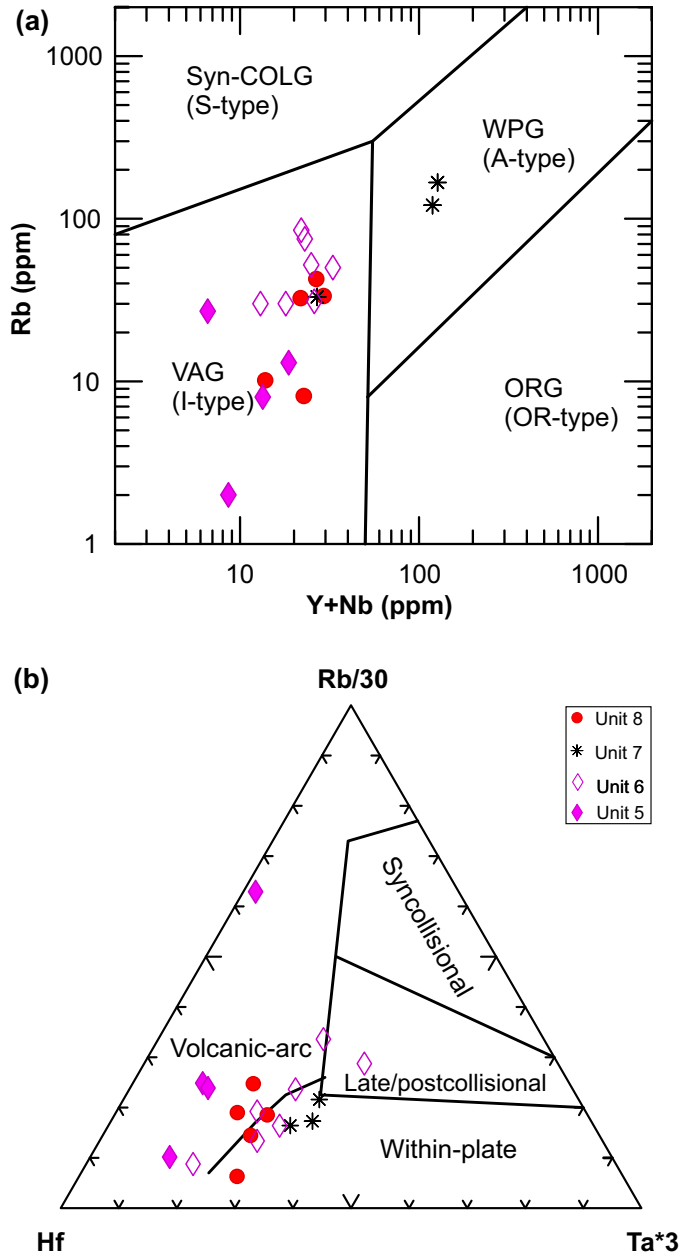

Figure GS2018-8-10: *Tectonomagmatic discrimination diagrams for units 5 to 8 intrusive rocks from the Farley Lake area:* ***a)*** *Rb (ppm) vs. (Y+Yb; ppm); the fields of ORG (ocean-ridge granitoids), syn-COLG (syncollision granitoids), VAG (volcanic-arc granitoids) and WPG (within-plate granitoids) are from Pearce et al. (1984) and correspond to the fields of OR-type, I-type, S-type and A-type granitoids, respectively, proposed by Christiansen and Keith (1996);* ***b)*** *Hf–Rb/30–Ta*3 ternary diagram (after Harris et al., 1986).*

resemble E-type MORB (0.29), whereas andesitic Sm/Nd ratios from unit 3b are similar to OIB (0.26; Sun and McDonough, 1989). These Sm/Nd ratios are consistent with the primitive-mantle–normalized, extended trace-element profiles (Figure GS2018-8-9), which suggest a volcanic-arc affinity (cf. Goldstein et al., 1984; Rollinson, 1993).

Similarly, $^{147}Sm/^{144}Nd$ isotopic ratios of the volcanic rocks in the Farley Lake area range from 0.1257 to 0.1761, and tend to increase with decreasing silica content (Table GS2018-8-2). The $^{143}Nd/^{144}Nd$ ratios range from 0.511960 to 0.512598. On a plot of $^{147}Sm/^{144}Nd$ versus $^{143}Nd/^{144}Nd$ ratios (Figure GS2018-8-11), the volcanic rock samples define a linear array that corresponds to an age of 1877 ±180 Ma with an initial $^{143}Nd/^{144}Nd$ ratio of 0.51039 ±0.00019 (ε_{Nd} = 3.6; Ludwig, 2008). The relatively large analytical uncertainty and MSWD of this regression are due largely to excess data-point scatter. Nevertheless, the Sm-Nd errorchron age is comparable to the TIMS U-Pb zircon age of 1884 Ma obtained for a unit 1a rhyo-

Table GS2018-8-2: Sm-Nd isotope composition of volcanic rocks from the Farley Lake area, Lynn Lake greenstone belt.

Sample	Easting[1]	Northing[1]	Rock type	Map unit[2]	Sm (ppm)	Nd (ppm)	Sm/ Nd	$^{147}Sm/^{144}Nd$	$^{143}Nd/^{144}Nd$	Uncert.*	εNd_0	T_{DM} (Ga)	T (Ma)	εNd_T
111-16-210A01	409596	6303716	Rhyolite	1	5.52	26.55	0.21	0.1257	0.511960	0.000007	-13.2	2.08	1884	4.0
111-16-220B01	411975	6309079	Aphyric andesite	3b	2.13	7.38	0.29	0.1743	0.512533	0.000006	-2.0	N/A	1884	3.4
111-16-318A01	409573	6297103	Amphibole-porphyroblastic andesite	3b	3.88	17.48	0.22	0.1344	0.512040	0.000007	-11.7	2.15	1884	3.4
111-16-203A01	413972	6306969	Plagioclase-phyric basalt	3c	3.60	12.95	0.28	0.1682	0.512460	0.000006	-3.5	N/A	1884	3.4
111-16-207A01	413710	6306883	Plagioclase-phyric andesite	3c	5.67	21.19	0.27	0.1617	0.512378	0.000007	-5.1	N/A	1884	3.4
111-16-215A01	412813	6309586	Plagioclase-phyric basalt	3c	1.35	4.63	0.29	0.1761	0.512598	0.000010	-0.8	N/A	1884	4.2

Notes:
[1] UTM Zone14N, NAD83
[2] Map units in Yang and Beaumont-Smith (2016b)
T_{DM} not calculated for samples with $^{147}Sm/^{144}Nd > 0.14$
All samples relative to La Jolla $^{143}Nd/^{144}Nd = 0.511850$
* Uncertainty is 2 σ abolute errors on $^{143}Nd/^{144}Nd$; estimated error of $^{147}Sm/^{144}Nd$ is better than 0.2%
T_{DM} uses the linear model of Goldstein et al. (1984)

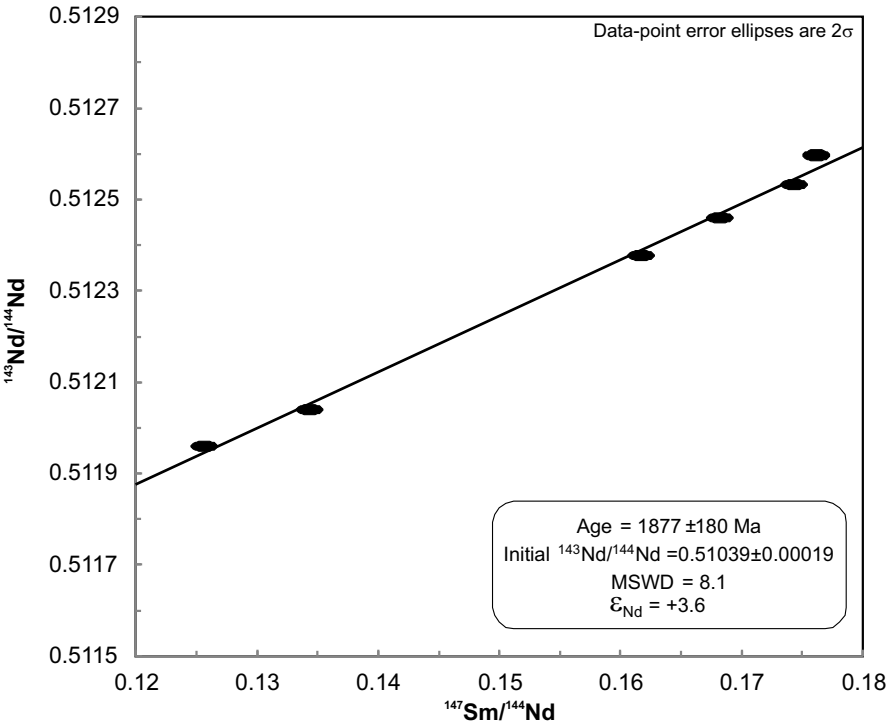

Figure GS2018-8-11: *Errorchron plot of $^{147}Sm/^{144}Nd$ vs. $^{143}Nd/^{144}Nd$ ratios for the Farley Lake volcanic rocks, Lynn Lake greenstone belt.*

lite sample (Beaumont-Smith, unpublished data, 2006; Yang and Beaumont-Smith, 2016a).

Figure GS2018-8-12 presents a time (t) versus ε_{Nd} evolution diagram for the 1884 Ma Farley Lake volcanic rocks. The evolution line of depleted mantle is based on Goldstein et al. (1984). Six samples of volcanic rocks from the Farley Lake area yielded ε_{Nd} values ranging from +3.4 to +4.2 at an age of 1884 Ma, suggesting that they are derived from a depleted mantle source and that crustal contamination was limited. The two dashed lines show the trend of ε_{Nd} values of the magmas since their separation from the depleted-mantle source at approximately 2.2 to 2.1 Ga (T_{DM}; Table GS2018-8-2). The juvenile Nd isotopic compositions, combined with their trace-element characteristics (e.g., slightly enriched, notable Nb, Ta and Ti anomalies), suggest that the Farley Lake volcanic rocks were emplaced into an island-arc environment (see the insets in Figure GS2018-8-12).

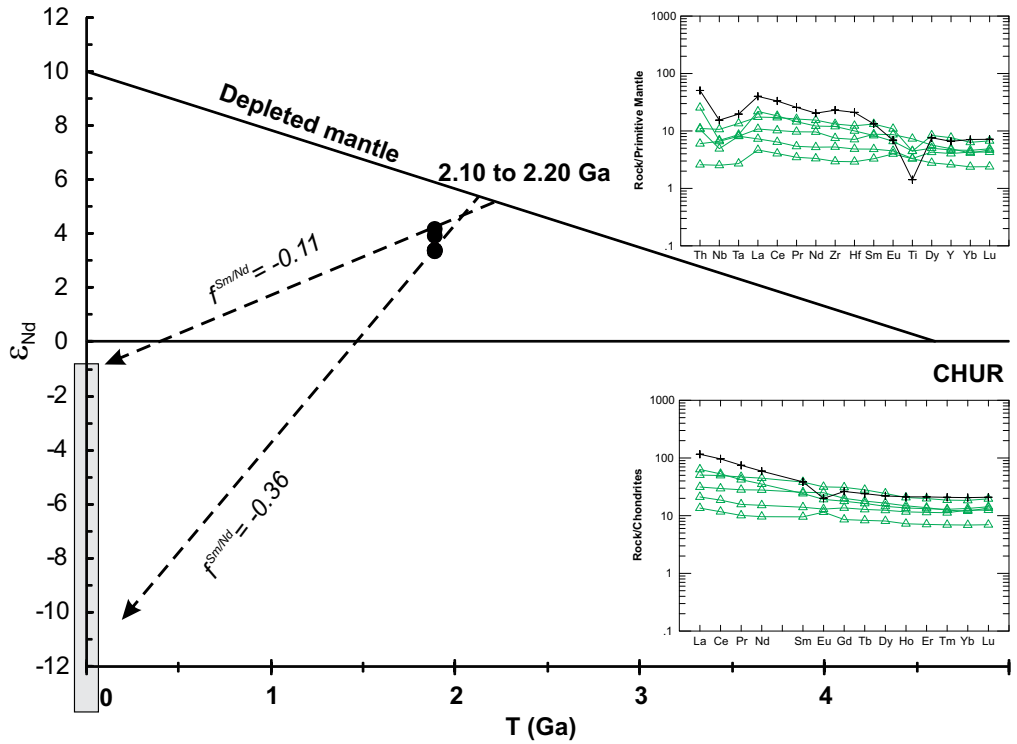

Figure GS2018-8-12: *Time (t) vs. ε_{Nd} evolution diagram for the 1.884 Ga Farley Lake volcanic rocks. Insets show the REE patterns and extended trace-element profiles of these six volcanic samples analyzed for Sm-Nd isotopes (Table GS2018-8-2). $f^{Sm/Nd}$ denotes fractionation factor (see Rollinson, 1993).*

SHRIMP U-Pb zircon dating

In order to establish timing of the various granitoid magmatism events in the Farley Lake area, three granitoid samples with distinctively different compositions were selected on the basis of field relationships for U-Pb zircon age determination using the sensitive high-resolution ion microprobe (SHRIMP) at the Geological Survey of Canada, Ottawa. Details about the method and data may be found in Lawley et al. (2018). Concordia diagrams for these samples are presented in Figure GS2018-8-13.

Sample 111-16-353A01 is a medium-grained granodiorite collected from a unit 6 granitoid pluton (Yang and Beaumont-Smith, 2016a) that intruded the volcanic and volcaniclastic rocks intercalated with metasedimentary rocks and BIF (Figure GS2018-8-2). Zircon grains recovered from this sample are prismatic to stubby and display oscillatory zoning. Concordant zircon grains yielded a weighted average $^{207}Pb/^{206}Pb$ age of 1879.4 ±4.3 Ma (Figure GS2018-8-13a). This age falls into the range for the 1890 to 1876 Ma Pool Lake plutonic suite (Baldwin et al., 1987; Beaumont-Smith and Böhm, 2002, 2003, 2004), implying that the granodiorite is part of the pre-Sickle intrusive suite (Yang and Beaumont-Smith, 2016a).

Sample 111-15-162A01 is a foliated, medium- to coarse-grained alkali-feldspar granite collected from a unit 7 granite intrusion that cuts unit 6 granitoid rocks (Yang and Beaumont-Smith, 2016a, b; Figure GS2018-8-2). Zircon grains retrieved from this sample display complex growth zoning, some with metasomatic domains. Concordant zircon grains yielded a weighted average $^{207}Pb/^{206}Pb$ age of 1872.6 ±2.5 Ma (Figure GS2018-8-13b), attributed to the pre-Sickle intrusive suite.

Sample 111-15-162A01 is a moderately foliated, medium-grained quartz diorite taken from a small stock that cuts mafic volcanic rocks and intercalated BIF at the south edge of the Gordon open pit (Figure GS2018-8-2). Zircon grains recovered from this sample are prismatic with typically oscillatory zonation. Concordant zircon grains yielded a weighted average $^{207}Pb/^{206}Pb$ age of 1854.4 ±2.4 Ma (Figure GS2018-8-13c). The age of the quartz diorite suggests that it could belong to the ca. 1865–1850 Ma Wathaman-Chipewyan plutonic suite (Corrigan et al., 2009).

Conclusions and economic considerations

Bedrock geological mapping, petrographic observations, lithogeochemical characterization and Sm-Nd

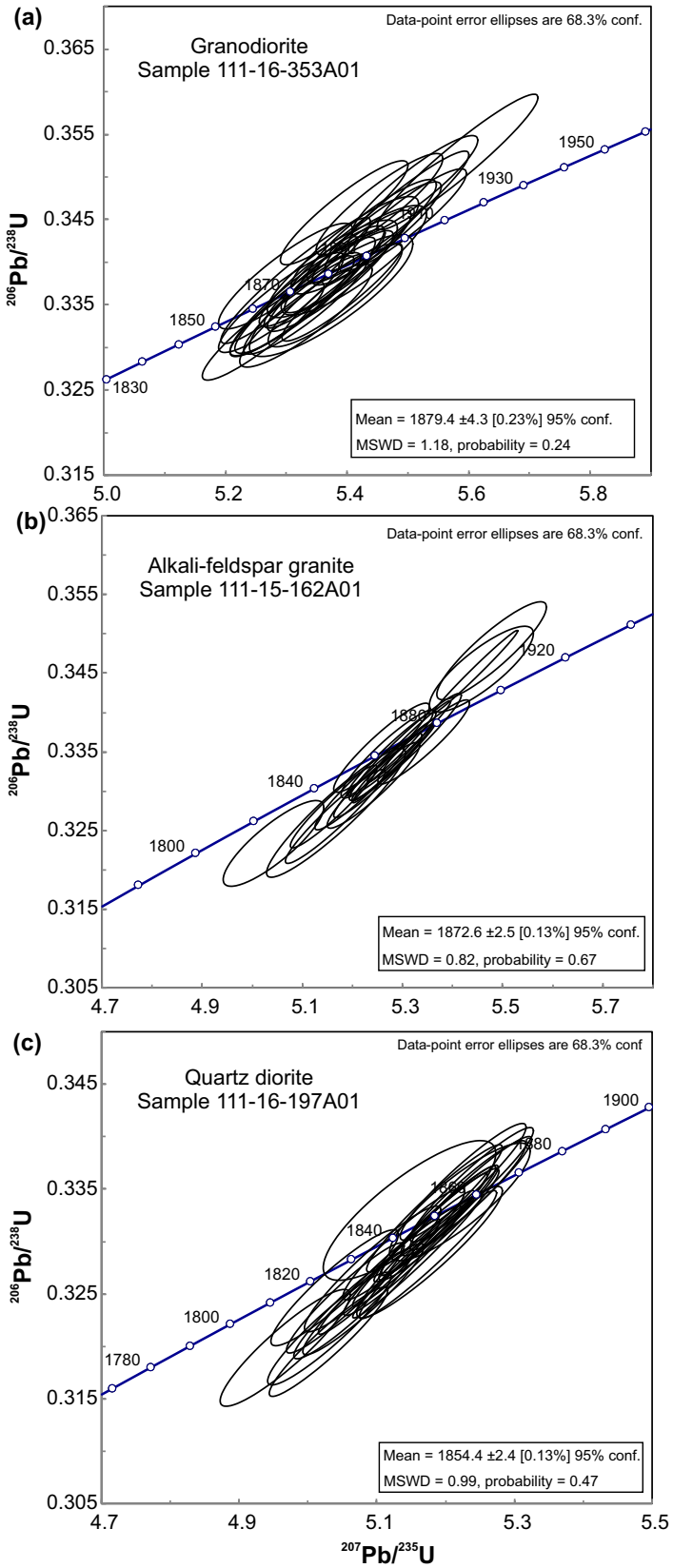

Figure GS2018-8-13: *Concordia diagram of sensitive high-resolution ion microprobe (SHRIMP) U-Pb zircon age data for granitoid samples from the Farley Lake area, Lynn Lake greenstone belt:* ***a)*** *unit 6 granodiorite, sample 111-16-353A01, UTM 412105E, 6306254N (Zone 14, NAD83);* ***b)*** *unit 7 alkali-feldspar granite, sample 111-15-162A01, UTM 411172E, 6301517N; and* ***c)*** *unit 8 quartz diorite, sample 111-16-197A01, UTM 412573E, 6307761N).*

isotopic results for volcanic rocks in the Farley Lake area provide clues to the origin and tectonic setting of the LLGB. Mafic to felsic volcanic rock samples yielded Sm/Nd ratios <1; enriched REE patterns; and extended trace-element profiles with notable, negative Nb, Ta and Ti anomalies. They follow a BADR compositional trend, suggesting that the volcanic (and sedimentary) rocks hosting the Gordon Au deposit in the Farley Lake area may have been deposited in an island-arc to back-arc tectonic setting.

Fine-grained interflow sediments, including BIF, argillite and lesser turbidite successions, are interpreted to be coeval with mafic to felsic volcanic rocks and likely mark volcanic hiatuses in a marine environment marginal to the active arc. An initial ε_{Nd} ratio of +3.6 for a suite of six, presumably cogenetic samples that yielded an errorchron age of 1877 ±180 Ma further suggests that a depleted mantle was the primary source of volcanism, which is in contrast to enriched, plume-like sources inferred for mafic volcanic rocks hosting the MacLellan Au-Ag deposit and elsewhere in the LLGB (Glendenning et al., 2015). The juvenile character of the Farley Lake volcanic rocks suggests that crustal contamination was limited, which is consistent with their interpreted island-arc setting and magma sourcing from a depleted mantle. Felsic to mafic volcanic rocks of the LLGB are also coeval with the subduction of the Manikewan ocean plate and may have been situated on the upper plate above a subduction zone (i.e., polarity to southeast) prior to the terminal stage of accretionary orogenesis with the Archean Hearn craton to the northwest (Hoffmann, 1988; Corrigan et al., 2007, 2009; Zwanzig and Bailes, 2010).

The SHRIMP U-Pb zircon ages, together with field relationships (Yang and Beaumont-Smith, 2016a, b), of granitoid rocks at Farley Lake indicate that supracrustal rocks were intruded by a successive suite of granitoid intrusions with distinct geochemistry. Pre-Sickle, volcanic-arc, I-type granodiorite likely intruded an immature to mature arc at ca. 1879 Ma, whereas the composition of ca. 1872 Ma granitic rocks (A-type) is more typical of an intra-arc extensional environment. These granitoids with different geochemical affinities suggest that intrusive rocks were structurally juxtaposed after emplacement, possibly during regional, main deformation at 1.81–1.80 Ga (see Beaumont-Smith and Böhm, 2002, 2003, 2004), and/or that disparate source regions were tapped at the same time within an evolving arc.

Younger (ca. 1854 Ma) adakite-like quartz diorite to monzodiorite are temporally and geochemically distinct from other granitoid rocks at Farley Lake. The composition of intermediate granitoids may be indicative of direct partial melting of the subducting slab and/or partial melting of prior metasomatized sub-arc lithospheric mantle due to instability within the mantle wedge after accretionary orogenesis but prior to ca. 1.83–1.80 Ga continent-continent collision between the Superior and Hearne cratons (Corrigan et al., 2009). Adakite-like intrusions, which are not related to older arc-type granitoid rocks, are known elsewhere as important hostrocks for some orogenic Au, intrusion-related Au, Fe oxide–Cu–Au and Carlin-type Au deposits (Groves et al., 2016). Intra-arc extensional settings represent favourable geological environments for Au concentration as late to postorogenic magmatism heated the crust and drove hydrothermal fluids.

Mapping reported here and previously, however, documents a pre-existing to synchronous deformation and metamorphic timing for an early generation of auriferous veins at the Gordon Au deposit. Peak metamorphism likely occurred at 1.81–1.80 Ga and continued until ca. 1.78 Ga, based on metamorphic zircon and/or monazite ages for the LLGB (Beaumont-Smith and Böhm, 2002, 2003, 2004; Lawley et al., 2018). Postdeformational veins were also reported from vein studies prior to flooding of the open pit at the Gordon Au deposit. The late timing of these veins and whether they contain Au are important questions that remain to be resolved. Nevertheless, the ca. 1854 Ma adakite-like intrusions predate the inferred timing of the earliest generation of auriferous veins by tens of millions of years. Adakite-like intrusions, therefore, represent an unlikely source for Au in the LLGB.

The spatial relationship between adakite-like intrusions and Au deposits in the LLGB, however, may still have economic significance. Adakite-like intrusions sampled within the open pit at the Gordon Au deposit, coupled with the distribution of other ca. 1.85 Ga plutons along the main Au-rich trend in the northern LLGB, suggest that auriferous fluids were focused along faults that reactivated the same structural architecture exploited by adakite-like intrusions. The most favourable faults for Au mineralization in the LLGB may therefore represent some of the earliest structures that juxtaposed the disparate volcanic and magmatic suites. Whether the distinct ca. 1.85 Ga magmatic event represents a favourable marker for Au in the LLGB and/or elsewhere in the Trans-Hudson orogeny, however, requires further study. In contrast, faults and favourable lithological assemblages that destabilize Au-S complexes within circulating hydrothermal fluids are clearly important and represent dominant ore-system controls at the Gordon Au deposit. The timing and source of auriferous fluids are the subject of ongoing

collaborative research between the MGS and the GSC via the TGI-5 program.

Acknowledgments

The authors thank C. Kovachik, J. Watts and E. Amyotte for providing enthusiastic and capable field assistance; E. Anderson and N. Brandson for thorough logistical support; and C. Epp for cataloguing, processing and preparing the samples. We thank T. Martins and C.O. Böhm for constructive reviews of the manuscript and R.F. Davie for technical editing of the report. Alamos Gold Inc. generously allowed access to its properties and drillcore facilities.

References

Anderson, S.D. 2013: Geology of the Garner–Gem lakes area, Rice Lake greenstone belt, southeastern Manitoba (parts of NTS 52L11, 14); Manitoba Mineral Resources, Manitoba Geological Survey, Geoscientific Report GR2013-1, 135 p.

Arndt, N.T. 2013: The formation and evolution of the continental crust; Geochemical Perspectives, v. 2, p. 405–533.

Ansdell, K.M. 2005: Tectonic evolution of the Manitoba-Saskatchewan segment of the Paleoproterozoic Trans-Hudson Orogen, Canada; Canadian Journal of Earth Sciences, v. 42, p. 741–759.

Ansdell, K.M., Corrigan, D., Stern, R. and Maxeiner, R. 1999: SHRIMP U-Pb geochronology of complex zircons from Reindeer Lake, Saskatchewan: implications for timing of sedimentation and metamorphism in the northwestern Trans-Hudson Orogen; Geological Association of Canada–Mineralogical Association of Canada, Joint Annual Meeting, Program with Abstracts, v. 24, p. 3.

Baldwin, D.A., Syme, E.C., Zwanzig, H.V., Gordon, T.M., Hunt, P.A. and Stevens, R.P. 1987: U-Pb zircon ages from the Lynn Lake and Rusty Lake metavolcanic belts, Manitoba: two ages of Proterozoic magmatism; Canadian Journal of Earth Sciences, v. 24, p. 1053–1063.

Baragar, W.R.A., Ernst, R.E., Hulbert, L. and Peterson, T. 1996: Longitudinal petrochemical variation in the Mackenzie dyke swarm, northwestern Canadian Shield; Journal of Petrology, v. 37, p. 317–359.

Bateman, J.D. 1945: McVeigh Lake area, Manitoba; Geological Survey of Canada, Paper 45-14, 34 p.

Beaumont-Smith, C.J. 2008: Geochemistry data for the Lynn Lake greenstone belt, Manitoba (NTS 64C11-16); Manitoba Science, Technology, Energy and Mines, Manitoba Geological Survey, Open File OF2007-1, 5 p.

Beaumont-Smith, C.J. and Böhm, C.O. 2002: Structural analysis and geochronological studies in the Lynn Lake greenstone belt and its gold-bearing shear zones (NTS 64C10, 11, 12, 14, 15 and 16), Manitoba; *in* Report of Activities 2002, Manitoba Industry, Trade and Mines, Manitoba Geological Survey, p. 159–170.

Beaumont-Smith, C.J. and Böhm, C.O. 2003: Tectonic evolution and gold metallogeny of the Lynn Lake greenstone belt, Manitoba (NTS 64C10, 11, 12, 14, 15 and 16), Manitoba; *in* Report of Activities 2003, Manitoba Industry, Economic Development and Mines, Manitoba Geological Survey, p. 39–49.

Beaumont-Smith, C.J. and Böhm, C.O. 2004: Structural analysis of the Lynn Lake greenstone belt, Manitoba (NTS 64C10, 11, 12, 14, 15 and 16); *in* Report of Activities 2004, Manitoba Industry, Economic Development and Mines, Manitoba Geological Survey, p. 55–68.

Beaumont-Smith, C.J., Machado, N. and Peck, D.C. 2006: New uranium-lead geochronology results from the Lynn Lake greenstone belt, Manitoba (NTS 64C11-16); Manitoba Science, Technology, Energy and Mines, Manitoba Geological Survey, Geoscientific Paper GP2006-1, 11 p.

Böhm, C.O., Zwanzig, H.V. and Creaser, R.A. 2007: Sm-Nd isotope technique as an exploration tool: delineating the northern extension of the Thompson Nickle Belt, Manitoba, Canada; Economic Geology, v. 102, p. 1217–1231.

Christiansen, E.H. and Keith, J.D. 1996: Trace-element systematics in silicic magmas: a metallogenic perspective; *in* Trace element geochemistry of volcanic rocks: applications for massive sulfide exploration, D.A. Wyman (ed.), Geological Association of Canada, Short Course Notes, no. 12, p. 115–151.

Chauvel, C., Arndt, N.T., Kielinzcuk, S. and Thom, A. 1987: Formation of Canadian 1.9 Ga old continental crust. I: Nd isotopic data; Canadian Journal of Earth Sciences, v. 26, p. 396–406.

Corrigan, D., Galley, A.G. and Pehrsson, S. 2007: Tectonic evolution and metallogeny of the southwestern Trans-Hudson Orogen; *in* Mineral Deposits of Canada: A Synthesis of Major Deposit-Types, District Metallogeny, the Evolution of Geological Provinces, and Exploration Methods, W.D. Goodfellow (ed.), Geological Association of Canada, Mineral Deposits Division, Special Publication 5, p. 881–902.

Corrigan, D., Pehrsson, S., Wodicka, N. and de Kemp, E. 2009: The Palaeoproterozoic Trans-Hudson Orogen: a prototype of modern accretionary processes; *in* Ancient Orogens and Modern Analogues, J.B. Murphy, J.D. Keppie, and A.J. Hynes (ed.), Geological Society of London, Special Publications, v. 327, p. 457–479.

Eby, G.N. 1990: The A-type granitoids: a review of their occurrence and chemical characteristics, and speculations on their petrogenesis; Lithos, v. 26, p. 115–134.

Fedikow, M.A.F. and Gale, G.H. 1982: Mineral deposit studies in the Lynn Lake area; *in* Report of Field Activities 1982, Manitoba Department of Energy and Mines, Mineral Resources Division, p. 44–54.

Frisch, W., Meschede, M. and Blakey, R. 2011: Plate tectonics: continental drift and mountain building. Springer, Heidelberg, 212 p.

Frost, B.R., Barnes, C.G., Collins, W.J., Arculus, R.J., Ellis, D.J. and Frost, C.D. 2001: A geochemical classification for granitic rocks; Journal of Petrology, v. 42, p. 2033–2048.

Gilbert, H.P. 1993: Geology of the Barrington Lake–Melvin Lake–Fraser Lake area; Manitoba Energy and Mines, Geological Services, Geological Report GR87-3, 97 p.

Gilbert, H.P., Syme, E.C. and Zwanzig, H.V. 1980: Geology of the metavolcanic and volcaniclastic metasedimentary rocks in the Lynn Lake area; Manitoba Energy and Mines, Mineral Resources Division, Geological Paper GP80-1, 118 p.

Glendenning, M.W.P., Gagnon, J.E. and Polat, A. 2015: Geochemistry of the metavolcanic rocks in the vicinity of the MacLellan Au-Ag deposit and an evaluation of the tectonic setting of the Lynn Lake greenstone belt, Canada: evidence for a Paleoproterozoic-aged rifted continental margin; Lithos, v. 233, p. 46–68.

Goldstein, S.L., O'Nions, R.K. and Hamilton, P.J. 1984: A Sm-Nd study of atmospheric dusts and particulates from major river systems; Earth and Planetary Science Letters, v. 70, p. 221–236.

Groves, D.I., Goldfarb, R.J. and Santosh, M. 2016: The conjunction of factors that led to formation of giant gold provinces and deposits in non-arc settings; Geoscience Frontiers, v. 7, p. 303–314.

Hoffman, P.H. 1988: United plates of America, the birth of a craton: Early Proterozoic assembly and growth of Laurentia; Annual Reviews of Earth and Planetary Sciences, v. 16, p. 543–603.

Harris, N.B.W., Pearce, J.A. and Tindle, A.G. 1986: Geochemical characteristics of collision-zone magmatism; *in* Collision Tectonics, M.P. Coward and A.C. Reis (ed.), Geological Society of London, Special Publications, v. 19, p. 67–81.

Hastie, E.C.G., Gagnon, J.E. and Samson, I.M. 2018: The Paleoproterozoic MacLellan deposit and related Au-Ag occurrences, Lynn Lake greenstone belt, Manitoba: an emerging, structurally controlled gold camp; Ore Geology Reviews, v. 94, p. 24–45.

Irvine, T.N. and Baragar, W.R.A. 1971: A guide to the chemical classification of the common volcanic rocks; Canadian Journal of Earth Sciences, v. 8, p. 523–548.

Kremer, P. D., Rayner, N. and Corkery, M.T. 2009: New results from geological mapping in the west-central and northeastern portions of Southern Indian Lake, Manitoba (parts of NTS 64G1, 2, 8, 64H4, 5); *in* Report of Activities 2009, Manitoba Science, Innovation, Energy and Mines, Manitoba Geological Survey, p. 94–107.

Lawley, C.J.M., Schneider, D., Yang, E., Davis, W.J., Jackson, S.E., Yang, Z., Zhang, S. and Selby, D. 2018: Age relationships and preliminary U-Pb zircon geochronology results from the Lynn Lake greenstone belt; *in* Targeted Geoscience Initiative: 2017 report of activities, volume 1, N. Rogers (ed.), Geological Survey of Canada, Open File 8358, p. 133–137.

Le Bas, M.J., Le Maitre, R.W., Streckeisen, A. and Zanettin, B. 1986: A chemical classification of volcanic rocks based on the total alkali silica diagram; Journal of Petrology, v. 27, p. 745–750.

Lewry, J.F. and Collerson, K.D. 1990: The Trans-Hudson Orogen: extent, subdivisions and problems; *in* The Early Proterozoic Trans-Hudson Orogen of North America, J.F. Lewry and M.R. Stauffer (ed.), Geological Association of Canada, Special Paper 37, p. 1–14.

Ludwig, K.R. 2008: User's manual for Isoplot 3.70: a geochronological toolkit for Microsoft Excel; Berkeley Geochronology Center, Special Publication 4, 76 p.

Maniar, P.D. and Piccoli, P.M. 1989: Tectonic discrimination of granitoids; Geological Society of America Bulletin, v. 101, p. 635–643.

Manitoba Energy and Mines 1986: Granville Lake, NTS 64C; Manitoba Energy and Mines, Minerals Division, Bedrock Geology Compilation Map Series, Map 64C, scale 1:250 000.

Martin, H., Smithies, R.H., Rapp, R., Moyen, J.-F. and Champion, D., 2005: An overview of adakite, tonalite-trondhjemite-granodiorite (TTG), and sanukitoid: relationships and some implications for crustal evolution; Lithos, v. 79, p. 1–24.

Meschede, M. 1986: A method of discriminating between different types of mid-ocean basalts and continental tholeiites with the Nb-Zr-Y diagram; Chemical Geology, v. 56, p. 207–218.

Milligan, G.C. 1960: Geology of the Lynn Lake district; Manitoba Department of Mines and Natural Resources, Mines Branch, Publication 57-1, 317 p.

Norman, G.W.H. 1933: Granville Lake district, northern Manitoba; Geological Survey of Canada, Summary Report, Part C, p. 23–41.

Moyen, J.-F. and Martin, H. 2012: Forty years of TTG research; Lithos, v. 148, p. 312–336.

Park, A.F., Beaumont-Smith, C.J. and Lentz, D.R. 2002: Structure and stratigraphy in the Agassiz Metallotect, Lynn Lake greenstone belt (NTS 64C/14 and /15), Manitoba; *in* Report of Activities 2002, Manitoba Industry, Trade and Mines, Manitoba Geological Survey, p. 171–186.

Pearce, J.A. 1996: A user's guide to basalt discrimination diagrams; *in* Trace Element Geochemistry of Volcanic Rocks: Applications for Massive Sulphide Exploration, D.A. Wyman (ed.), Geological Association of Canada, Short Course Notes, no. 12, p. 79–113.

Pearce, J.A. 2008: Geochemical fingerprinting of oceanic basalts with applications to ophiolite classification and the search for Archean oceanic crust; Lithos, v. 100, p. 14–48.

Pearce, J.A., Harris, N.B.W. and Tindle, A.G. 1984: Trace element discrimination diagrams for the tectonic interpretation of granitic rocks; Journal of Petrology, v. 25, p. 956–983.

Pearce, J.A. and Peate, D.W. 1995: Tectonic implications of the composition of volcanic arc magmas; Annual Review of Earth and Planetary Sciences, v. 23, p. 251–285.

Richards, J.P. and Kerrich, R. 2007: Special paper: dakite-like rocks: their diverse origins and questionable role in metallogenesis; Economic Geology, v. 102, p. 537–576, URL <https://doi.org/10.2113/gsecongeo.102.4.537> [November 2018].

Rittmann, A. 1973: Stable mineral assemblages of igneous rocks; Springer-Verlag, Berlin, 262 p.

Rollinson, H.R. 1993: Using geochemical data: evaluation, presentation, interpretation; Routledge, Taylor & Francis Group, London and New York, 352 p.

Rudnick, R.L. and Gao, S. 2003: Composition of the continental crust; Treatise on Geochemistry, v. 3, p. 1–64.

Shirey, S.B. and Hanson, G.N. 1984: Mantle-derived Archaean monozodiorites and trachyandesites; Nature, v. 310, p. 222–224.

Stauffer, M.R. 1984: Manikewan: an Early Proterozoic ocean in central Canada, its igneous history and orogenic closure; Precambrian Research, v. 25, p. 257–281.

Stern, R., Hanson, G.N. and Shirey, S.B. 1989: Petrogenesis of mantle derived LILE-enriched Archaean monzodiorite, trachyandesites (sanukitoids) in southern Superior Province; Canadian Journal of Earth Sciences, v. 26, p. 1688–1712.

Stern, R.A., Syme, E.C. and Lucas, S.B. 1995: Geochemistry of 1.9 Ga MORB- and OIB-like basalts from the Amisk collage, Flin Flon Belt, Canada: evidence for an intra-oceanic origin; Geochimica et Cosmochimica Acta, v. 59, p. 3131–3154.

Streckeisen, A.L. and LeMaitre, R.W. 1979: A chemical approximation to modal QAPF classification of the igneous rocks; Neues Jahrbuch für Mineralogie, v. 136, p. 169–206.

Sun, S.-s. and McDonough, W.F. 1989: Chemical and isotopic systematics of oceanic basalts: implications for mantle composition and processes; *in* Magmatism in the Ocean Basins, A.D. Saunders and M.J. Norry (ed.), Geological Society of London, Special Publications, v. 42, p. 313–345.

Syme, E.C. 1985: Geochemistry of metavolcanic rocks in the Lynn Lake Belt; Manitoba Energy and Mines, Geological Services, Geological Report GR84-1, 84 p. plus 1 map at 1:100 000 scale.

Turek, A., Woodhead, J. and Zwanzig H.V. 2000: U-Pb age of the gabbro and other plutons at Lynn Lake (part of NTS 64C); *in* Report of Activities 2000, Manitoba Industry, Trade and Mines, Manitoba Geological Survey, p. 97–104.

Whalen, J.B., Currie, K.L. and Chappell, B.W. 1987: A-type granites: geochemical characteristics, discrimination and petrogenesis; Contributions to Mineralogy and Petrology, v. 95, p. 407–419.

Whalen, J.B. and Frost, C.D. 2013: The Q-ANOR diagram: a tool for the petro-genetic and tectonomagmatic characterization of granitic suites; URL <https://www.researchgate.net/publication/290161821> [September 2018].

Wood, D.A. 1980: The application of a Th-Hf-Ta diagram to problems of tectonomagmatic classification and to establishing the nature of crustal contamination of basaltic lavas of the British Tertiary volcanic province; Earth and Planetary Science Letters, v. 50, p. 11–30.

Yang, X.M. 2007: Using the Rittmann Serial Index to define the alkalinity of igneous rocks; Neues Jahrbuch für Mineralogie, v. 184, p. 95–103.

Yang, X.M. and Beaumont-Smith, C.J. 2015: Geological investigations of the Keewatin River area, Lynn Lake greenstone belt, northwestern Manitoba (parts of NTS 64C14, 15); *in* Report of Activities 2015, Manitoba Mineral Resources, Manitoba Geological Survey, p. 52–67.

Yang, X.M. and Beaumont-Smith, C.J. 2016a: Geological investigations in the Farley Lake area, Lynn Lake greenstone belt, northwestern Manitoba (part of NTS 64C16); *in* Report of Activities 2016, Manitoba Growth, Enterprise and Trade, Manitoba Geological Survey, p. 99–114.

Yang, X.M. and Beaumont-Smith, C.J. 2016b: Bedrock geology of the Farley Lake area, Lynn Lake greenstone belt, northwestern Manitoba (part of NTS 64C16); Manitoba Growth, Enterprise and Trade, Manitoba Geological Survey, Preliminary Map PMAP2016-5, scale 1:20 000.

Yang, X.M. and Beaumont-Smith, C.J. 2017: Geological investigations of the Wasekwan Lake area, Lynn Lake greenstone belt, northwestern Manitoba (parts of NTS 64C10, 15); *in* Report of Activities 2017, Manitoba Growth, Enterprise and Trade, Manitoba Geological Survey, p. 117–132.

Zwanzig, H.V., Syme, E.C. and Gilbert, H.P. 1999: Updated trace element geochemistry of ca. 1.9 Ga metavolcanic rocks in the Paleoproterozoic Lynn Lake belt; Manitoba Industry, Trade and Mines, Geological Services, Open File Report OF99-13, 46 p.

Zwanzig, H.V. and Bailes, A.H. 2010: Geology and geochemical evolution of the northern Flin Flon and southern Kisseynew domains, Kississing–File lakes area, Manitoba (parts of NTS 63K, N); Manitoba Innovation, Energy and Mines, Manitoba Geological Survey, Geoscientific Report GR2010-1, 135 p.